Monthly Notices of the ROYAL ASTRONOMICAL SOCIETY
MNRAS **522,** 3588–3601 (2023) https://doi.org/10.1093/mnras/stad1124

Resequencing the Hubble sequence and the quadratic (black hole mass)–(spheroid stellar mass) relation for elliptical galaxies

Alister W. Graham ★
OzGrav-Swinburne, Centre for Astrophysics and Supercomputing, Swinburne University of Technology, Hawthorn, VIC 3122, Australia

Accepted 2023 April 13. Received 2023 April 13; in original form 2023 February 20

ABSTRACT

One of the most protracted problems in astronomy has been understanding the evolution of galaxy morphology. Much discussion has surrounded how lenticular galaxies may form a bridging population between elliptical and spiral galaxies. However, with recourse to a galaxy's central black hole mass, accretion-built spiral galaxies have emerged as the bridging population between low-mass lenticular galaxies and the dusty merger-built lenticular galaxies contiguous with elliptical galaxies and 'brightest cluster galaxies' in the black hole/galaxy mass diagram. Spiral galaxies, including the Milky Way, appear built from gas accretion and minor mergers onto what were initially lenticular galaxies. These connections are expressed as a new morphology sequence, dubbed the 'Triangal', which subsumes elements of the Hubble sequence and the van den Bergh trident and reveals the bridging nature of the often overlooked ellicular galaxies. Furthermore, a quadratic black hole/galaxy mass relation is found to describe ordinary elliptical galaxies. The relation is roughly parallel to the quadratic-like relations observed for the central spheroidal component of spiral galaxies, dust-rich lenticular galaxies, and old dust-poor lenticular galaxies. The brightest cluster galaxies are offset according to expectations from an additional major merger. The findings have implications for feedback from active galactic nuclei, mapping morphology into simulations, and predicting gravitational wave signals from colliding supermassive black holes. A new galaxy speciation model is presented. It disfavours the 'monolithic collapse' scenario for spiral, dusty lenticular, and elliptical galaxies. It reveals substantial orbital angular momentum in the Universe's first galaxies and unites dwarf and ordinary 'early-type' galaxies.

Key words: galaxies: bulges – galaxies: elliptical and lenticular, cD – galaxies: evolution – galaxies: interactions – (galaxies:) quasars: supermassive black holes – galaxies: structure.

1 INTRODUCTION

Since the first spiral 'nebula' was discovered (Rosse 1850), astronomers have pondered their formation and connection with other nebulae (Alexander 1852; Roberts 1895; Aitken 1906; Jeans 1919). Indeed, how the extragalactic nebulae, the 'island universes'[1] of Curtis (1917), nowadays referred to as galaxies, may evolve and transform from their primordial incarnation remains an active and open topic of research (e.g. Boselli & Gavazzi 2006; Park, Gott & Choi 2008; van den Bosch et al. 2008; Cameron & Pettitt 2012; Conselice 2014; Schawinski et al. 2014). With roots in the 1700s, today's most well-known galaxy sequence was stripped of its evolutionary pathways almost as soon as it was conceived a century ago. As revealed in the well-referenced papers by Hart & Berendzen (1971) and Way (2013), see also Graham (2019b), credit for the E-to-S (Hubble 1926) and E-S0-S (Hubble 1936) 'Hubble sequence' resides with many.

Jeans (1919) popularised the notion of amorphous round/elliptical-shaped nebulae evolving into ringed/spiral nebulae. Such a concept originated from the 18th century 'nebular hypothesis' in which elliptical-shaped nebulae were thought to rotate and throw-off rings and spiral arms at the expense of a dwindling central bulge. Building on this, Reynolds (1920) introduced the essence of the early-to-late type spiral sequence, based in part[2] on the dominance of the bulge, with this central concentration later adopted as criteria by Lundmark (1925, 1926) and Hubble (1926). The notion of an initial (early) and latter (late) type of nebulae was initially entertained by Hubble[3]

★ E-mail: AGraham@astro.swin.edu.au

[1] von Humboldt (1845) used the German word Weltinsel (world island) to refer to our Galaxy and everything floating in space. Mädler (1846) subsequently referred to the nebulae as 'world islands', which Mitchel (1847) translated and adapted into 'island universes'.

[2] An additional facet was the appearance of condensations in the arms. This facet stemmed from earlier speculation that planets may condense out of material ejected from nebulae, and thus a more granulated appearance reflected a more evolved system. As Hart & Berendzen (1971) note, in 1923, Hubble embraced this idea, along with noting the presence/absence of a spiral galaxy's bar, as previously reported by Curtis (1918).

[3] As noted by Hart & Berendzen (1971), in 1923, in preparation for the second International Astronomical Union, Hubble submitted a manuscript to Slipher in which he wrote 'there is some justification in considering the elliptical nebulae as representing an earlier stage of evolution' and he also now listed them *before* the spiral nebula, reversing the spiral-spindle/ovate order in his original scheme (Hubble 1922).

but later disfavoured by many in the early-to-mid 1920s, including Hubble (1926). Nonetheless, the early- and late-type nomenclature was retained. The practice of quantifying the roundness of a 'regular' nebula—encompassing the early-type galaxies—with designations ranging from 1 for round nebulae to 5 for elongated nebulae had been used since Herschel (1847). While Hubble expanded upon this practice, he also sought to distil the key elements from the detailed scheme of Wolf (1908).[4] Furthermore, Curtis (1918) had recently introduced the barred versus non-barred designation following the murky identification of bars by Knox-Shaw (1915). This led to the bifurcation of the S galaxies that Hubble (1926) included in his first table. Hart & Berendzen (1971, their footnote 42) and van den Bergh (1997) remind us that Jeans (1928) was the first to express this visually, as a Y-shaped diagram before Hubble (1936) turned it sideways to give us the so-called `tuning fork', with the intermediary spindle/lenticular class, i.e. the armless disc galaxies introduced by Reynolds (1925), being the S0 galaxies at the junction.

The longevity of the Jeans/Reynolds/Hubble sequence of galaxies, encapsulated by the tuning fork – taught in most introductory astronomy courses – is perhaps surprising given that doubt over the direction of potential morphological transformations led Hubble (1926) to recant that this was an evolutionary sequence (Hart & Berendzen 1971). However, a wealth of additional characteristics was subsequently grafted onto and coded in by de Vaucouleurs (1959) and Buta, Corwin & Odewahn (2007), and this does reflect some of the formation histories of galaxies (Buta 2013).

While some galaxies, and their spheroidal component, are known to be built by collisions (e.g. Naab & Burkert 2003; Merritt 2006; Conselice et al. 2022), vital clues from the coevolution of their massive black holes (BHs) have only now come to light. It has recently been revealed how gas-poor, aka 'dry,' mergers of S0 galaxies (Reynolds 1925; van den Bergh 2009) have created the offset population of E galaxies (including brightest cluster galaxies, BCGs) in the diagram of BH mass, $M_{\rm bh}$, versus spheroid[5] stellar mass, $M_{*,\rm sph}$ (Graham & Sahu 2023a). The merger-induced transition of stars from ordered rotating discs in S0 galaxies into a somewhat chaotic 'dynamically hot' spheroidal-shaped swarm, coupled with the steep $M_{\rm bh}$–$M_{*,\rm sph}$ mass scaling none relation for S0 galaxies, explains why, at a given mass, the E galaxies have an order-of-magnitude lower $M_{\rm bh}/M_{*,\rm sph}$ ratio than the S0 galaxies, as first observed by Sahu, Graham & Davis (2019a).

Feedback from 'active galactic nuclei' (e.g. Salpeter 1964; Silk & Rees 1998; Heckman & Best 2014) has typically been heralded as the driving force behind the BH/galaxy scaling relations (e.g. Magorrian et al. 1998; Ferrarese & Merritt 2000; Gebhardt et al. 2000; Graham et al. 2001), with the initially small scatter about the $M_{\rm bh}$-(stellar velocity dispersion, σ) relation taken as proof. However, it is now apparent that dry mergers, rather than BH feedback, have dictated the behaviour of the E galaxies in the $M_{\rm bh}$–$M_{*,\rm sph}$ diagram (Graham & Sahu 2023a). Furthermore, the virial theorem, coupled with the best measurements of spheroid size and stellar mass, has revealed how dry mergers explain why the $M_{\rm bh}$–σ relation does not have much scatter at the high-mass end where the E galaxies reside (Graham 2023a).

Inspecting *Hubble Space Telescope* (*HST*) images available at the Hubble Legacy Archive (HLA),[6] it has also recently been revealed that there are two populations of S0 galaxy: dust-poor and dust-rich (Graham 2023b). Based on the results in Appendix A, this may mirror a division previously detected as low- and high-luminosity S0 galaxies (van den Bergh 1990), which needed to be explained and integrated into a joint evolutionary and galaxy morphology classification scheme. The existence of two populations helps explain a century of confusion, different formation scenarios, and physical properties for S0 galaxies (Aguerri 2012). The dusty S0 galaxies are major-merger remnants that involved gas and star formation, referred to as 'wet' mergers. As the star formation fades, these S0 galaxies will migrate across the 'green valley' and on to the 'red sequence' in diagrams of colour versus stellar mass (Powell et al. 2017). The S galaxies are observed to reside between the dust-poor and dust-rich S0 galaxies in the $M_{\rm bh}$–$M_{*,\rm sph}$ diagram. Furthermore, the S galaxies are known to have been built, or rather renovated, by minor mergers, which may encompass the accretion of gas clouds from surrounding HI (e.g. Block et al. 2007; Cluver et al. 2010; Wang et al. 2015), the devouring of satellite galaxies, and the capture of dwarf galaxies (e.g. Searle & Zinn 1978; Pickering et al. 1997; Gallagher 2010; Garling et al. 2018; Li et al. 2018; Kruijssen et al. 2019; Mao et al. 2021). While such gravitational disturbances may invoke a spiral pattern (Julian & Toomre 1966), too large a merger is likely to dynamically overheat the disc, destroy or prevent any spiral, and produce a dusty S0 galaxy such as NGC 3108 (Hau et al. 2008) or Centaurus A (Ebneter & Balick 1983), which, in time, may resemble something more like the Sombrero galaxy.

Given that the BCGs are likely to be E galaxies built by multiple mergers (e.g. Laine et al. 2003), the E galaxy population is explored more thoroughly here. The BCGs may be offset in the $M_{\rm bh}$–$M_{*,\rm sph}$ diagram from the (non-BCG, or simply 'ordinary') E galaxies. An offset will not be observed if the E galaxies follow the near-linear $M_{\rm bh}$-$M_{*,\rm sph}$ relation they have been thought to follow for a quarter of a century (Magorrian et al. 1998; Kormendy & Ho 2013; Saglia et al. 2016). However, for a steeper than linear non-BCG E galaxy $M_{\rm bh}$–$M_{*,\rm sph}$ relation, the addition of two ordinary E galaxies' stars and their central BH would lead to a merger-induced jump, referred to as 'punctuated equilibrium' (Graham & Sahu 2023a),[7] taking them off the ordinary E galaxy $M_{\rm bh}$–$M_{*,\rm sph}$ relation. This jump is detected here, and, for the first time, all of the merger-built morphological transformations are shown to map into a triangular-like diagram revealing fundamental connections between the galaxy types. The 'Triangal', presented herein, supersedes the Hubble sequence by (i) redrawing the connections and (ii) including evolutionary pathways. It is, nonetheless, a development based on the works of many, in particular van den Bergh (1976, 1990).

2 DATA: ORDINARY ELLIPTICAL GALAXIES VERSUS BCGS

The data for this investigation consists of published BH masses, spheroid (and galaxy) stellar masses, and the galaxies' morphological

[4]While the nebulae classification scheme of Wolf (1908) is not in use, Charles Wolf is remembered through Wolf–Rayet stars (Wolf & Rayet 1867), the central stars of *planetary* nebulae (Wright 1914).

[5]Here, the spheroidal component of a galaxy refers to either a central bulge of a disc galaxy or the bulk of an E galaxy.

[6]https://hla.stsci.edu/

[7]As Graham & Sahu (2023a) noted, the phrase 'punctuated equilibrium' stems from studies of Darwinian evolution. Eldredge & Gould (1972) proposed that species are stable until a rare and rapid event occurs. For a galaxy, such an event could be represented by a substantial merger, resulting in significant evolutionary change. Within evolutionary biology, such branching speciation is called cladogenesis.

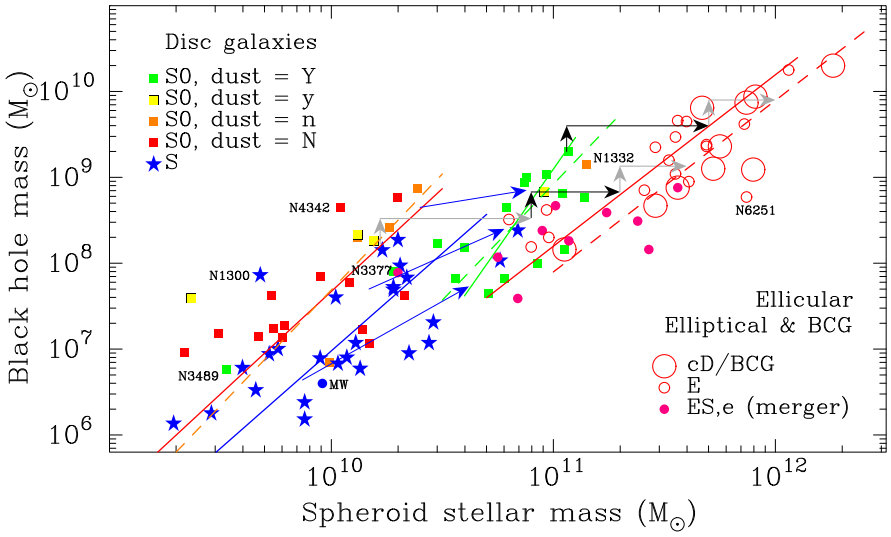

Figure 1. Morphologically-aware $M_{\rm bh}$–$M_{*,\rm sph}$ diagram. The ten cD and BCG (including the dusty S0 galaxy NGC 1316 and the ES,e galaxy NGC 1275), along with NGC 3377 and NGC 6251, were excluded from the fit to the (remaining) 24 E/ES,e galaxies (right-most solid red line: equation 1). The one BCG above this line is NGC 4486. The (non-BCG) E galaxy with the highest BH mass is NGC 1600. The dashed red line represents the BCG. The lines for the (S0 and S) disc galaxies have come from (Graham 2023b). Using the S0 galaxy 'dust bins' (Graham 2023b), the left-most red solid line represents S0 galaxies without visible signs of dust (dust = N), while the orange dashed line additionally includes S0 galaxies with only a nuclear dust disc or ring (dust = n). The green dashed line is the orange dashed line shifted horizontally by an arbitrary log (3.5) ≈ 0.54 dex, while the solid green line is a fit to the dusty (dust = Y) S0 galaxies, excluding those with only a little widespread dust (dust = y). The blue line represents the S galaxy data. Labelled galaxies were excluded from the Bayesian analyses. From left to right, the logarithmic slopes are: 2.39 ± 0.81 (red line); 2.70 ± 0.77 (dashed orange line); 2.27 ± 0.48 (blue line); 3.69 ± 1.51 (solid green line); 2.70 ± 0.77 (dashed green line); and 2.00 ± 0.25 (red solid and dashed line). Full equations are in Table 1, and the arrows are explained in the main text.

type, including whether the E galaxies are BCG or cD[8] (Graham & Sahu 2023a,b), and S0 galaxy 'dust bin' (Graham 2023b). For ease of reference, the cD and BCG will often collectively be referred to as BCG in the text. The spheroid masses were obtained from careful[9] multicomponent decompositions, which separate bars and inner discs from spheroids and other galaxy components. X/(peanut shell)-shaped structures were captured by a Fourier analysis of the isophotal shapes (Carter 1978; Ciambur 2015; Ciambur & Graham 2016) and effectively folded back into the bar component. As such, components that some may call a 'pseudobulge' or a false bulge are not considered the spheroid. The spheroid may, however, have a Sérsic index of less than 2 ± 0.5, a divide that has been questioned (e.g. Graham 2013, 2019a). For each galaxy, the decomposition has been plotted and published (Savorgnan & Graham 2016; Davis, Graham & Cameron 2019; Sahu et al. 2019a; Graham & Sahu 2023b).

3 RESULTS

The current focus explores separating the spheroid-dominated E and ES,e galaxies[10] into BCGs and non-BCGs (Graham & Sahu 2023b). Given that galaxy groups can be small in number (3–5), a brightest group galaxy (BGG) may be an ordinary E galaxy, a dusty S0 galaxy or occasionally an S galaxy if no major merging has occurred. As such, the BGG tend not to not distinguish themselves in the $M_{\rm bh}$–$M_{*,\rm sph}$ diagram. As indicated in Section 1, the author has been evolving this diagram piecewise to make the changes more digestible and to better emphasise the importance of galaxy morphology and origin. Readers familiar with only a single regression line in this diagram may like to review fig. 1 in Graham & Sahu (2023b), which separates the galaxies into S, S0, and E types, and fig. 4 in Graham (2023b), which further separates the S0 galaxies into dust-poor and dust-rich bins. These 'dust bins' or classes are illustrated in fig. 1 of Graham (2023b).[11] In what follows, the BCGs (most of which are E galaxies) are separated from the ordinary (non-BCG) E galaxies.

Fig. 1 shows the ordinary E galaxies (including the ES,e galaxies described and identified in Graham & Sahu 2023b) and 10 BCGs in the $M_{\rm bh}$–$M_{*,\rm sph}$ diagram. Due to their ability to skew the result, two apparent outliers – NGC 3377 (ES,e) and NGC 6251 (E), which are marked in Fig. 1 and discussed in Appendix B along

[8]cD galaxies may be the first or second brightest galaxy in a cluster. They have a centrally-dominant location, and as such, they are immersed at the centre of the intracluster light, which appears as a diffuse halo (Conroy, Wechsler & Kravtsov 2007).

[9]Rather than blindly fitting multiple Sérsic functions, (galaxy component)-specific functions were fit after inspecting the images and consulting with the literature, including kinematic maps.

[10]Ellicular (ES) galaxies (Liller 1966) are spheroid-dominated but have fully embedded discs. Also known as 'disc ellipticals' (Nieto, Capaccioli & Held 1988), Buta et al. (2015, their table 1) referred to them as S0$^-$ sp/E5-E7 and presented a dozen examples in their fig. 23. They typically have spheroid-to-total stellar mass ratios around ∼0.9 ± 0.05 (Graham & Sahu 2023a), and there might be two species (Graham & Sahu 2023b). The ES,b galaxies have spheroids more akin to the bulges of S0 galaxies, and the four in the current sample are treated as such here. They may be relics from the early merging of the now-dust-poor S0 galaxies with high bulge-to-total stellar mass ratios (B/T), or old spheroid-dominated systems which only accreted an intermediate-scale disc. The ES,e galaxies have spheroids more like E galaxies, and are likely built from the merger of dusty S0 and/or gas-poor S galaxies.

[11]A more quantitative approach could involve the specific dust mass (e.g. Engelbracht et al. 2008), i.e. the dust mass normalised by the stellar mass, but one may still need to pay attention to nuclear dust discs versus wide-spread dust.

with other interesting outliers – are excluded from the Bayesian analysis (method described in Davis et al. 2019) performed here on the ordinary E and ES,e galaxies. This analysis yields[12]

$$\log(M_{\rm bh}/{\rm M}_\odot) = (2.00 \pm 0.25)[\log(M_{*,\rm sph}/{\rm M}_\odot) - 11.32] + (8.84 \pm 0.15). \quad (1)$$

This quadratic relation is dramatically different to the near-linear relation previously thought to define the coevolution of E galaxies and their BHs (Magorrian et al. 1998).

The bulk of the 10 BCGs are seen to reside to the right of equation (1) in Fig. 1. This is readily explained if, on average, they predominantly formed from the major merger of two E or ES,e galaxies. The situation could equally represent the merger of several S0 galaxies or some other suitable combination. The steeper than linear nature of the ordinary E/ES,e $M_{\rm bh}$–$M_{*,\rm sph}$ relation (equation 1) results in dry mergers forming BCGs that reside to the right of, rather than on, equation (1). More data are required to obtain a reliable fit for the distribution of the BCGs. Therefore, a simple mass doubling from a major dry merger has been used to define the dashed red line in Fig. 1, which appears broadly representative of the distribution of the BCGs.

Differing from the single S0 galaxy $M_{\rm bh}$–$M_{*,\rm sph}$ relation presented in Graham & Sahu (2023a), the S0 galaxies are placed in four 'dust bins' following Graham (2023b). These bins are denoted as follows: N for no visible dust; n for only a nuclear dust disc/ring; y for weak widespread dust; and Y for strong, widespread dust features. As alluded to in the Introduction, this was established in Graham (2023b) by looking at colour images in the HLA. Roughly, nuclear discs are less than a few hundred parsecs in (radial) size, while widespread features may be 2 to 3 or more kpc in (radial) size. To a certain degree, one can expect a general sequence of increasing dust from the low-mass S0 galaxies to the spiral galaxies and on to the (wet merger)-built S0 galaxies, some of which were previously ultraluminous infrared galaxies (ULIRGs: Komossa et al. 2003; Dasyra et al. 2006). This stems from the trickle of star formation in spiral galaxies and the starbursts that formed the dusty S0 galaxies, in which metals condensed out of the interstellar medium.

The dust-poor S0 galaxies need not be gas-poor, and some may contain expansive HI envelopes (e.g. van Zee, Haynes & Giovanelli 1995). Massive reservoirs of hydrogen gas are known to surround some low-mass and low surface brightness galaxies (e.g. Hoffman et al. 1993; Impey & Bothun 1997; Blitz & Robishaw 2000). Low surface brightness galaxies are also known to be metal-poor (e.g. McGaugh 1994). Such gas clouds may remain indefinitely unless an angular-momentum-robbing gravitational disturbance drives them inwards to fuel a galactic metamorphosis or a passing neighbour leads to a gas bridge. These gas clouds could instead be removed via several well-known mechanisms within a group or cluster environment. The latter processes will leave a dust-poor S0 galaxy, while the first may build an S galaxy. In passing, it is noted that a dust-poor S0 galaxies' present-day mass function of stars will be a truncated and modified form of the initial mass function from 10 to 13 Gyr ago. With stellar mass-loss due to winds and supernovae ejecta, coupled with ram-pressure stripping within a group/cluster environment, the galaxies' stellar masses will reduce over time. Thus, the stellar orbits within the galaxies' discs will slightly expand from their initial configuration. Coupled with a faded stellar population, the surface brightnesses will be reduced. That is, this 'bloating' (in the plane) of the disc – after consumption of the available gas at the formation epoch – adds to the dimness of local ($z \sim 0$) low surface brightness and ultra-diffuse disc galaxies (and dwarf spheroidal-shaped galaxies).

[12]Including NGC 6251 gives a logarithmic slope of 1.90 ± 0.25, while including NGC 3377 and NGC 6251 gives a logarithmic slope of 1.65 ± 0.22.

Table 1. $M_{\rm bh}$–$M_{*,\rm sph}$ and $M_{\rm bh}$–$M_{*,\rm gal}$ relations.

Galaxy type	N	slope (A)	mid-pt (C)	intercept (B)	$\Delta_{\rm rms}$
$\log(M_{\rm bh}/{\rm M}_\odot) = A[\log(M_{*,\rm sph}/\upsilon\,{\rm M}_\odot) - C] + B$ (Fig. 1)					
S0 (dust = N)	13	2.39 ± 0.81	9.90	7.43 ± 0.18	0.58
S0 (dust = n,N)	17	2.70 ± 0.77	9.96	7.57 ± 0.18	0.61
S	25	2.27 ± 0.48	10.09	7.18 ± 0.15	0.52
S0/Es,b (dust = Y)*	15	2.70 ± 0.77	9.96	6.11 ± 0.18	0.52
E/Es,e	24	2.00 ± 0.25	11.32	8.84 ± 0.14	0.36
BCG*	10	2.00 ± 0.25	11.32	8.54 ± 0.14	0.31
$\log(M_{\rm bh}/{\rm M}_\odot) = A[\log(M_{*,\rm gal}/\upsilon\,{\rm M}_\odot) - C] + B$ (Appendix A)					
E/Es,e	24	2.06 ± 0.26	11.35	8.85 ± 0.15	0.37
E/ES,e/S0(dust = Y)	39	2.27 ± 0.25	11.27	8.69 ± 0.11	0.43
BCG*	09	2.27 ± 0.25	11.27	8.39 ± 0.11	0.36
$\log(M_{\rm bh}/{\rm M}_\odot) = A[\log(M_{*,\rm gal}/\upsilon\,{\rm M}_\odot) - C] + B$ (Appendix A)					
major mergers	48	2.07 ± 0.19	11.37	8.83 ± 0.10	0.41
S	25	2.68 ± 0.46	10.79	7.17 ± 0.14	0.52
S (w/o Circinus)	24	3.04 ± 0.59	10.81	7.21 ± 0.14	0.47
S0/Es,b (dust = Y)	15	2.65 ± 0.54	11.08	8.30 ± 0.20	0.52

Note. The sample size, N, of each galaxy type is given in Column 2. The type 'major mergers' includes the BCG, the ordinary E/ES,e galaxies, and the S0 galaxies with dust = Y. The relations are derived from a Bayesian analysis that treats the data symmetrically rather than minimising the root mean square (rms) scatter, $\Delta_{\rm rms}$ dex, about the fitted relation in the BH direction. An asterisk (∗) on the galaxy type indicates an estimated rather than measured relation (see Fig. 1 and the Appendix A). The υ term equals 1.0 here and whenever using stellar mass estimates consistent with those derived from equation (4) in Graham & Sahu (2023a).

In Fig. 1, relations for the S0 galaxies with either no dust or strong dust features are included for reference with the relation for non-BCG E galaxies. Equations are provided in Table 1.

Connected with the B/T ratios, several $M_{\rm bh}$–$M_{*,\rm gal}$ relations are shown in Appendix A. As no galaxy decompositions are required, these may be more amenable for studying ensembles of BH mergers and the associated ocean of gravitational waves they produce (Shannon et al. 2015; Goncharov et al. 2021; Amaro-Seoane et al. 2023).

4 DISCUSSION

4.1 Making tracks

Fig.1 reveals several $M_{\rm bh}$–$M_{*,\rm sph}$ scaling relations, illustrating the march of galaxies to larger masses and different morphological types. There are fitted relations for non-dusty S0 galaxies (Graham 2023b), S galaxies (Davis et al. 2019; Graham & Sahu 2023a), and ordinary E/ES,e galaxies (equation 1). In addition is the trend for dusty S0 galaxies (Graham 2023b), which is offset from the relation defined by non-dusty S0 galaxies, and the trend for BCGs, which we have just seen is offset from the relation defined by the non-BCG E/ES,e galaxies. Collectively, the adjacent relations track a sequence of increasing chaos, albeit with spirals blooming along the way. The increasing entropy, revealed through the growth of 'dynamically hot' spheroids at the expense of ordered rotating discs, results in convergence towards pure E galaxies. This evolution between and along the relations could be quantified with a chaos parameter, such as the B/T stellar mass ratio or dynamical mass ratio: $\sigma^2 R_{\rm sph}/V^2 h_{\rm disc}$,

where $R_{\rm sph}$ is a suitable radius for the spheroid, V is the disc rotation at some outer radius, and $h_{\rm disc}$ is the disc scale-length.

The relatively dust-poor S0 galaxies on the left-hand side of Fig. 1 might be quasi-primordial if frozen in time due to a cluster environment which stripped away their gas, eroded their satellites, and inhibited galaxy mergers due to high-speed passages within the cluster swarm. In contrast, the dusty S0 galaxies may be built from wet S+S mergers (lower blue arrow) and wet S0+S mergers (middle and upper blue arrows). Such mergers can result in gas clouds shocking against each other, falling inwards to perhaps form a new disc, and sparking galaxy-centric bursts of dusty star formation. The relatively cool atmospheres of asymptotic giant branch stars rich in carbon and oxygen, or exploding supernovae, previously sprayed metals into the interstellar medium. Initially, most of these elements stay in a gas phase, although some quickly condense into dust particles as the stellar winds/ejecta expand and cool. These refractory dust grain cores can grow substantial mantles as they enter dense metal-enriched gas clouds within the cooling interstellar medium (Draine 2003). Indeed, the high metallicity, high dust content, and high density of neutral gas will aid the gas cooling, molecule formation, and cloud condensation. A sequence of increasing dust-to-HI with metallicity, [O/H], can be seen in, for example, Engelbracht et al. (2008, their fig. 6). The result is a somewhat distinct population of dusty, high-mass S0 galaxies.

The few dust-poor S0 galaxies overlapping with the S galaxies might be former S galaxies (Rathore et al. 2022), which have lost their dust, gas, and spiral density wave due to entering a harsh cluster environment (Yagi et al. 2010). Their satellites may then effectively evaporate, thereby contributing to the intracluster light rather than building up (the bulge of) the central galaxy (Conroy et al. 2007). Such evolution, or rather stagnation, is often expressed in terms of S galaxies fading to become S0 galaxies.

Finally, the grey and black arrows in Fig. 1 denote major dry mergers, in which $M_{*,\rm sph}$ can increase more than $M_{\rm bh}$ if some of the progenitor galaxies' disc stars get folded into the newly wedded galaxy's spheroidal component. These arrows show transitions from S0 to E to BCG (the upper set of arrows) and from S0 to ES,e to E to BCG (the lower set of arrows). For example, the black arrow pair above NGC 1322 reflects a major dry merger of two S0 galaxies with a B/T ratio of 0.5; the end product represents a doubling of the BH mass and a quadrupling of the spheroid stellar mass. The merger remnant is an E galaxy if the orbital angular momentum cancels. Should the net angular momentum of the system not cancel, then the system will not make it across to the E sequence but fall short, forming either an ES galaxy with an intermediate-scale disc or an S0 galaxy with a dominant disc. Once a galaxy's stellar mass is great enough, at $M_* > \sim 10^{11}$ M$_\odot$, it is not uncommon for galaxies to be immersed in a million-degree corona, which destroys and removes the dust and cooler star-forming gas (Benson et al. 2003; Draine 2003, 2004; McNamara & Nulsen 2012).

Overlaying the galaxies' morphological type onto the $M_{\rm bh}$–$M_{*,\rm sph}$ diagram has painted a new picture of the accretion history of galaxies. This augmented scaling diagram reveals the major mergers, such as the (i) transition from dust-poor S0 galaxies to dusty S0 galaxies built from wet mergers and having high $M_{*,\rm gal}/M_{\rm bh}$ ratios, (ii) the dry merger of S0 galaxies to produce ES and E galaxies, and (iii) the merger of E galaxies (and massive S0 galaxies) to produce BCG. Furthermore, the $M_{\rm bh}$–$M_{*,\rm sph}$ diagram suggests that gas accretion and minor mergers onto dust-poor S0 galaxies have created the spiral galaxies. A cleaner representation of the data and tracks in Fig. 1 is summarised through a simplified schematic in Fig. 2. It captures the major trends and transitions. This is also shown pictorially in

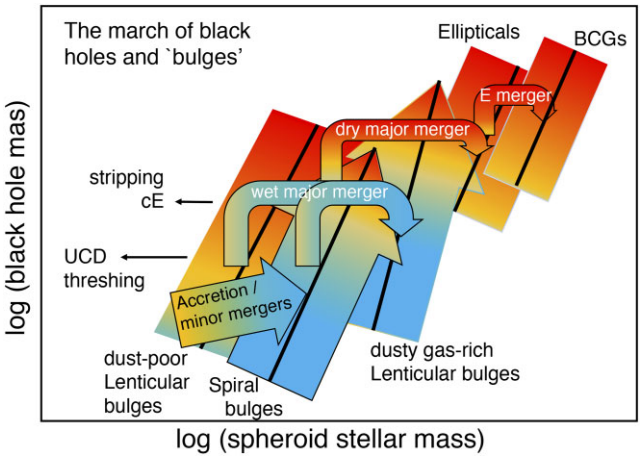

Figure 2. Morphologically-aware $M_{\rm bh}$–$M_{*,\rm sph}$ schematic. The progression of BH mass and 'bulge' mass, i.e. the stellar mass of the spheroidal component of galaxies.

Fig. 3. The S galaxy NGC 4151 shown there is a Seyfert with faint, wispy arms extending beyond the displayed frame. It is reminiscent of UGC 6614 (not in sample), which has a low surface brightness disc with extended wispy arms and a prominent bulge with an active galactic nucleus (Schombert 1998; Das et al. 2006). UGC 6614 is HI-rich and may have partially grown by accreting a dwarf galaxy (Pickering et al. 1997).

For the S galaxies, the spiral-arm winding angle correlates with the BH mass (Seigar et al. 2008; Davis, Graham & Seigar 2017), offering a view of the changing S galaxy morphology along the S galaxy $M_{\rm bh}$–$M_{*,\rm sph}$ relation. The low-mass S galaxies with low B/T ratios (see Appendix A) tend to have loosely wound spiral arms, while the opposite is observed at high masses. The spiral patterns in S galaxies form in discs; that is, a disc is first required. The formation of the S galaxies, sandwiched between the dust-poor and dust-rich S0 galaxies in the $M_{\rm bh}$–$M_{*,\rm sph}$ diagram suggests that gas accretion and minor mergers may be required for their emergence. A consequence is that our Milky Way galaxy was likely an S0 galaxy in the past before it merged with the *Gaia*-Sausage-Enceladus satellite galaxy 10 Gyr ago. However, if the mass ratio of merging galaxies is too close to 1, the outcome may be more destructive, producing an S0 galaxy like Centaurus A. Indeed, such an outcome is expected when the Milky Way eventually collides with the Andromeda galaxy in several Gyr (van der Marel et al. 2012; Eingorn et al. 2013; Schiavi et al. 2020)[13].

Suppose the more massive of the original, currently dust-poor, S0 galaxies had more satellites than the lower mass dust-poor S0 galaxies – akin to the increased numbers of dark matter subhaloes observed in simulations (Moore et al. 1999; Ishiyama et al. 2013). In that case, then satellite capture and integration into the central S0 galaxy may build more massive bulges in the more massive dust-poor S0 galaxies. Such growth may also contribute to the trend of the B/T ratio along the (Sa-Sb-Sc) S galaxy sequence (Graham & Worley 2008) and, in turn, contribute to a tightening of the winding of the spiral arms generated by the density waves (Lin & Shu 1964). Such *harvesting* of satellites may help complete the picture of galaxy evolution, explaining why Sa galaxies have bigger B/T ratios than the less massive Sc galaxies and perhaps partly explaining the missing

[13]Given the expected dusty nature of the merger product, a more apt name than ``Milkomeda" may be ``Dustomeda".

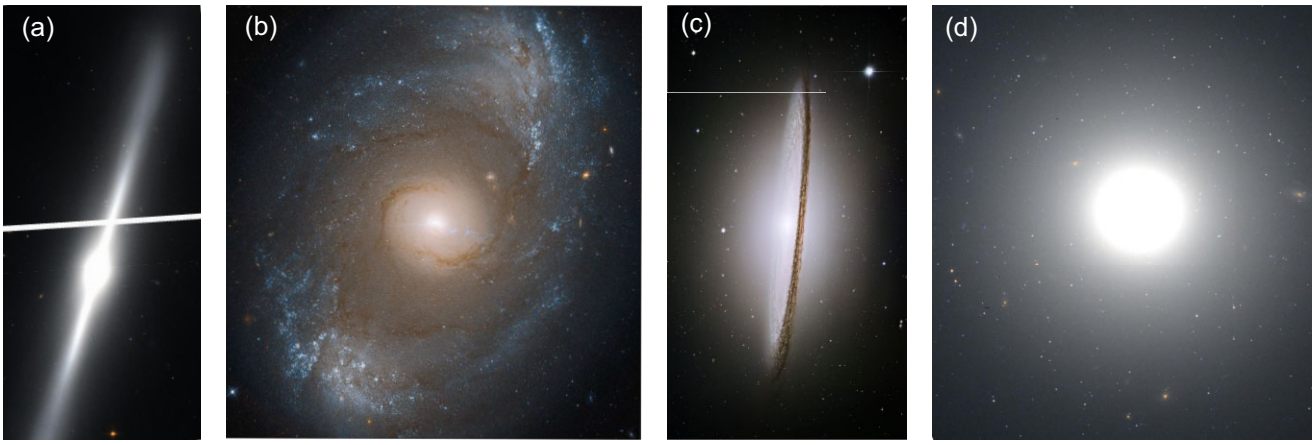

Figure 3. Intergalactic speciation. Panel a: Dust-poor S0 galaxy NGC 4762 (HST Prop. 9401. PI. P.Cote. F850LP/F475W ACS/WFC). Panel b: S galaxy NGC 4151 (HST Prop. 13765. PI. B.Peterson. F814W/F350LP WFC3/UVIS. Credit: STScI/NASA, ESA, Joseph DePasquale). Panel c: Dust-rich S0 galaxy NGC 4594 (Credit: NASA and the Hubble Heritage Team. STScI/AURA). Panel d: E galaxy NGC 1407 (HST Prop. 9427. PI. W.Harris. F814W/F435W ACS/WFC). The white stripe in panel A is due to the camera join.

satellite problem (D'Onghia et al. 2010). The merger-driven galaxy evolution revealed by the BH mass scaling diagrams (Fig. 1) should also aid our understanding of the (dark matter halo mass)–(galaxy stellar mass) relations as a function of galaxy type (Brouwer et al. 2021; Posti & Fall 2021).

Due to dynamical friction (Chandrasekhar & von Neumann 1943; Baranov & Batrakov 1974; Tremaine, Ostriker & Spitzer 1975; Inoue 2011; Arca-Sedda & Capuzzo-Dolcetta 2014b), albeit with competing evaporative effects (Ostriker, Binney & Saha 1989; Madrid et al. 2017), the currently dust-poor S0 galaxies that once resided, and may still reside, in richer globular clusters system are expected to have imprisoned more globular clusters at their centre (Capuzzo-Dolcetta 1993). They should, therefore, contain a more massive nuclear star cluster (Arca-Sedda & Capuzzo-Dolcetta 2014a; Leaman & van de Ven 2022). Unlike in gas-poor globular clusters, BHs can feed and grow at the centres of galaxies – and perhaps rapidly so (Davies, Miller & Bellovary 2011) –, and a (black hole)–(nuclear star cluster) mass relation exists (Graham 2020). This relation may have its origins in the dust-poor S0 galaxy sequence.

4.2 Acquisitions and mergers

Almost as soon as the first S galaxy was discovered (Rosse 1850), it was suggested that a tidal encounter with another galaxy might produce spiral-like 'tidal arms' (Roche 1850; Alexander 1852; Aitken 1906; Hoyle 1951). In addition, infalling perturbers may induce a (transient, Sellwood 2011; Baba et al. 2018) spiral pattern (Julian & Toomre 1966; Dubinski et al. 2008; Kazantzidis et al. 2009) or a bar (Steinmetz & Navarro 2002) – which may aid some longer-lasting grand-design spirals – and provide gas for ongoing star formation. To date, the Milky Way galaxy appears to have had at least one significant merger 10 Gyr ago, with the *Gaia* Sausage-Enceladus satellite (Helmi et al. 1999; Belokurov et al. 2018; Helmi et al. 2018; Gallart et al. 2019), and perhaps an even greater merger before that (Horta et al. 2021). This is in addition to many increasingly lesser mergers involving, for example, the Sagittarius and Canis Major satellite galaxies (Martínez-Delgado et al. 2001; Kruijssen et al. 2019), and perhaps explaining Gould's Belt (Bekki 2009a). Indeed, data from the ESA *Gaia* satellite has revealed that the disc of our Galaxy is notably unsettled (Antoja et al. 2018; Gaia Collaboration et al. 2018; Bland-Hawthorn & Tepper-García 2021). Furthermore, disrupted dwarf or satellite galaxies are now routinely seen around S galaxies (Martínez-Delgado et al. 2008, 2010; Javanmardi et al. 2016; Mao et al. 2021).

The extent to which the low-mass S0 galaxies have 'harvested' systems from their neighbourhood, and undergone star formation, could be substantial given the factor of four difference in galaxy stellar mass seen between the dust-poor S0 galaxies and the spiral galaxies at fixed BH mass (see Appendix A). However, there may have been considerable retardation of growth in the dust-poor S0 galaxies located in clusters, and groups, due to a curtailed supply of gas and stripping of stars (Gunn & Gott 1972; Kawata & Mulchaey 2008; Bekki 2009b). Furthermore, the early-type spiral (Sa/Sb) galaxies with big bulges may have been built by a major merger followed by disc-building (Steinmetz & Navarro 2002; Hammer et al. 2009). In contrast, the ES,b galaxies may not have experienced the subsequent disc re-growth that these early-type S galaxies did.

It stands to reason that our Milky Way galaxy, perhaps first recognised as a spiral system 170yr ago (Alexander 1852, see also Scheiner 1899), was not born as an S galaxy but was previously an S0 galaxy. This conclusion is supported by a myriad of stellar chemical and kinematic information (Matsuno, Aoki & Suda 2019; Di Matteo et al. 2020). The abundance of disc galaxies seen at high redshifts by Ferreira et al. (2022) using the *James Webb Space Telescope* (*JWST*) also supports a picture of early disc galaxy formation. S galaxies would then consist of an old S0 galaxy disc, in which a thin disc has formed, and a spiral emerged (Yuan et al. 2017), albeit with the ongoing competition with mergers (and spiral arms) which can dynamically heat and thicken a disc (Toth & Ostriker 1992; Dubinski et al. 2008; Kawata et al. 2018). It would be interesting to learn, through JWST observations, when the spiral patterns formed in the S0 galaxies, presumably marking when a cold gas disc formed and a density wave emerged from the differential rotation of the galaxy disc.

Cosmological simulations reveal an abundance of satellites contributing to the growth of galaxies (e.g. Chua et al. 2017; Engler et al. 2021; Dillamore et al. 2022). The star cluster Nikhuli, in the disturbed S galaxy NGC 4424, is thought to represent the remains of a disrupted dwarf early-type galaxy that may be delivering a BH into NGC 4424 (Graham et al. 2021), and potentially generating

gravitational waves should a second massive BH already reside there (Brown et al. 2007; Mandel & Gair 2009). Perhaps the *Gaia* Sausage-Enceladus satellite stream also contained a migrant BH brought into our Galaxy.

In Fig. 4, the dS0 galaxies are added to the low-mass end of the dust-poor S0 (not S) galaxy sequence, where one observes the spiralless disc galaxies with small bulges and $M_{*,\rm gal} < 10^{10}{\rm M}_{\odot}$ (see Appendix A). If galaxies like IC 335, NGC 4452, and NGC 5866 (not in sample) are edge-on, near-bulgeless S0 galaxies, then some face-on examples may resemble low surface brightness galaxies, including ultra-diffuse galaxies (UDGs; Sandage & Binggeli 1984; Henkel et al. 2017). They may follow the curved size-(stellar mass) relation for early-type galaxies (Graham 2019a) to lower masses and larger galaxy half-light radii.[14] Some dS0 galaxies have been detected with faint spiral arms (Jerjen, Kalnajs & Binggeli 2000; Barazza, Binggeli & Jerjen 2002; Graham, Jerjen & Guzmán 2003b). Rather than being faded dwarf S galaxies, which are rare (Sandage & Binggeli 1984), they may be dwarf lenticular (dS0) galaxies attempting the transition to a late-type S galaxy (Corbin & Vacca 2002; Graham et al. 2017) but retarded by lower numbers of satellites and reduced gas accretion.

5 PLACING DEVELOPMENTS IN CONTEXT

One of the most well-known diagrams in astronomy is the 'Hubble sequence' also known as the 'Hubble tuning fork', reviewed in Graham (2019b) along with other galaxy morphology schemata. The sequence was initially thought to be evolutionary, based on the 'nebular hypothesis' from the 1700s. A legacy of that hypothesis is the 'early-type' and 'late-type' galaxy nomenclature used over the past century for the E/S0 and S galaxies, respectively, plus the early- and late-type spiral galaxy designation (e.g. Lundmark 1925, p.867), Originally, the Sa/Sb galaxies were thought to form before the Sc/Sd galaxies (Jeans 1919; Reynolds 1921, 1925). The S0 galaxies were introduced later and positioned before the Sa galaxies, or rather, between the E and Sa galaxies to give the sequence: (E0-E3)-S0-(Sa-Sc), where the ellipticity of the E galaxies is denoted by $1 - b/a$, with b/a the observed axis ratio and thus apparently round galaxies labelled E0. However, in terms of an increasing mass build-up, Fig. 1 (and Fig. A2) reveals how one encounters the so-called `late-type S' galaxies (Sc/Sd), known to have smaller BH masses, before the 'early-type S' galaxies (Sa/Sb), known to have larger BH masses. Although, within the 'down-sizing' scenario (Cowie et al. 1996), the higher mass S galaxies might finish forming first.

This section provides a brief overview of the significant advances which have led to the emergence of a new, triangular-like galaxy sequence presented in Fig. 4 and detailed further in Fig. A1. Dubbed the 'Triangal,' it reveals the morphological connections and, for the first time, the merger-induced evolutionary pathways responsible for galactic speciation. It identifies, and recognises the significance of, the dust-poor and dust-rich S0 galaxies.

Fig. 4 reflects that a galaxy's collisional record is evident from its morphology. As for the underlying, merger-driven, morphology-dependent $M_{\rm bh}$–$M_{*,\rm sph}$ scaling relations, BHs may now seem somewhat akin to passengers, carried along by major mergers in which the redistribution of disc stars, and the increase in orbital entropy, leads to the step-change creation, i.e. 'punctuated equilibrium,' of more massive spheroids and the transition to a new species of galaxy. Major wet mergers are, however, also associated with star formation and BH growth. Gaseous processes may be restricted to producing movement along the individual quadratic or steeper $M_{\rm bh}$–$M_{*,\rm sph}$ relations, yielding a kind of 'gradualism' rather than evolution off any morphology-dependent relation.

Derived from the morphologically-aware $M_{\rm bh}$–$M_{*,\rm sph}$ diagram (Fig. 1), the schematic in Fig. 4 capture elements of not just the 'Hubble sequence' but also the van den Bergh trident, introduced within the Revised David Dunlap Observatory system (van den Bergh 1976), which was later re-expressed as the ATLAS$^{\rm 3D}$ comb (Cappellari et al. 2011). Since the van den Bergh trident was introduced, there have been several significant developments, two of which trace back to work by Sidney van den Bergh. First was the realisation that many early-type galaxies contain discs (Capaccioli 1990; Rix & White 1990) such that low-luminosity[15] early-type galaxies are S0 galaxies rather than E galaxies (van den Bergh 1990). The abundance of rotating discs was later witnessed through kinematic information (Graham et al. 1998; Emsellem et al. 2011). Second was the realisation that there are two subtypes of S0 galaxy: low- and high-luminosity (van den Bergh 1990), with the origin of the high-luminosity S0 galaxies now known to be due to wet mergers (Graham 2023b). These dusty high-luminosity S0 galaxies are not faded S galaxies (Spitzer & Baade 1951) – an idea which partly motivated the van den Bergh trident (van den Bergh 1976) – but S+S (Bekki 1998; Naab & Burkert 2003; Querejeta et al. 2015) or S+S0 or (cold-gas rich but dust-poor) S0+S0 merger remnants. This accounts for why they are more massive than the S galaxy population (van den Bergh 1990; Burstein et al. 2005). The sequence of dust-poor S0 galaxies seen in Fig. 1 are also not faded S galaxies but rather failed S galaxies that never were.

The S0 galaxies are not the lynchpin they were initially thought to be (Reynolds 1925; Hubble 1936); that description seems more apt of the ES galaxies (Liller 1966), which are both 'fast rotators' and 'slow rotators,' backtracking on themselves in the modified spin-ellipticity diagram for galaxies (Bellstedt et al. 2017). The ES galaxies are a bridging population between the E and S0 galaxies, while the S galaxies are now a bridging population between the dust-poor and dust-rich S0 galaxies.

Recognising that S0 galaxies are not simply a single bridging population (E0-E3)-S0-(Sa-Sc), nor are they a single low-(spiral strength) side to the disc galaxy distribution of B/T ratio and spiral strength (van den Bergh 1976), alleviates a long-standing mystery. While the dusty S0 galaxies are a merger-built bridging population between the S and E galaxies, the non-dusty S0 galaxies form both a low-mass extension of the E galaxies – along a sequence of changing B/T ratio and specific angular momentum (Bender 1988; Capaccioli & Caon 1992) – and provide a population for accretion, minor mergers, and the development of spiral structures.

In addition to the B/T ratio (Fig. A2) – known to correlate with the bulge mass (e.g. Graham & Worley 2008) – future work will explore the location in the $M_{\rm bh}$–$M_{*,\rm sph}$ diagram of S galaxies with different arm strengths (van den Bergh 1976). After checking if systems with weak/anaemic arms preferentially reside on one side of the S galaxy sequence, the location of disc galaxies with strong/weak/no bars (de Vaucouleurs 1959) will be examined. Furthermore, it may be insightful to explore if other features, such as ring-shape versus spiral-shape (de Vaucouleurs 1959) or the wealth of fine detail captured by the 'Comprehensive de Vaucouleurs revised Hubble-

[14] In the absence of a centrally concentrated bulge, the galaxy size becomes the disc size.

[15] Absolute magnitude $M_B > -20$ mag, $\rm H_0 = 50\ km\ s^{-1}\ Mpc^{-1}$.

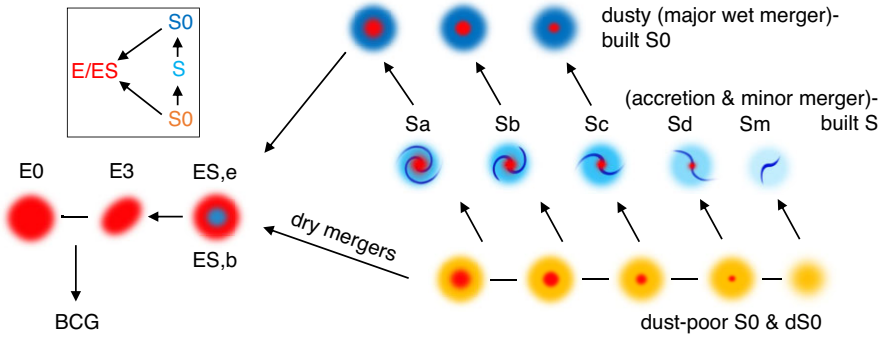

Figure 4. Not quite a regular three-pointed triangle, the 'Triangal' (derived and simplified in Fig. A1) reproduces elements of past galaxy morphology schemata (Hubble 1936; van den Bergh 1976; Cappellari et al. 2011), recognises the ES galaxies, includes merger remnants, no longer presents the S0 galaxies as only a bridging population between the E and S galaxies, connects the dwarf and dust-poor S0 galaxies with each other, and reveals the accretion and merger-driven evolutionary paths between the morphological types. Spheroids are coloured red, while large-scale discs are coloured orange (old metal-poor/dust-poor), cyan (enriched with young metal-rich population), and blue (enriched/dusty). The intermediate-scale discs in different ES galaxies have a range of stellar populations.

Sandage' system (Buta et al. 2007), occur in galaxies preferentially occupying a specific part of the diagram.

ACKNOWLEDGEMENTS

This paper is dedicated to the memory of Troy Charles Smith (1973 February 8 – 2023 February 2), a great friend and neighbour to interact with, and whose ``but what about...'' queries would prompt one to rethink the status quo.

The author warmly thanks Drs Denis W. Coates and Vale Keith Thompson, formerly at Monash University, for past discussions.

Part of this research was conducted within the Australian Research Council's Centre of Excellence for Gravitational Wave Discovery (OzGrav) through project number CE170100004. This work has used the NASA/IPAC Infrared Science Archive (IRSA), the NASA Extragalactic Database (NED), NASA's Astrophysics Data System (ADS) Bibliographic Services, and the HLA.

DATA AVAILABILITY

The data for this investigation consists of published (Graham & Sahu 2023a) black hole masses, spheroid (and galaxy) stellar masses, along with the galaxies' morphological type, including whether the E galaxies are BCG or cD(Graham & Sahu 2023b). The spheroid masses are obtained from published multicomponent decompositions, which separate bars and inner discs from the spheroids(Savorgnan & Graham 2016; Davis et al. 2019; Sahu et al. 2019a; Graham & Sahu 2023b).

REFERENCES

Abadi M. G., Navarro J. F., Steinmetz M., Eke V. R., 2003, ApJ, 597, 21
Adibekyan V. Z., Sousa S. G., Santos N. C., Delgado Mena E., González Hernández J. I., Israelian G., Mayor M., Khachatryan G., 2012, A&A, 545, A32
Aguerri J. A. L., 2012, Adv. Astron., 2012, 382674
Aitken R. G., 1906, PASP, 18, 111
Alexander S., 1852, AJ, 2, 97
Amaro-Seoane P. et al., 2023, Living Rev. Rel., 26, 2
Antoja T. et al., 2018, Nature, 561, 360
Arca-Sedda M., Capuzzo-Dolcetta R., 2014a, MNRAS, 444, 3738
Arca-Sedda M., Capuzzo-Dolcetta R., 2014b, ApJ, 785, 51
Baba J., Kawata D., Matsunaga N., Grand R. J. J., Hunt J. A. S., 2018, ApJ, 853, L23
Bajaja E., van der Burg G., Faber S. M., Gallagher J. S., Knapp G. R., Shane W. W., 1984, A&A, 141, 309
Baranov A. S., Batrakov Y. V., 1974, Soviet Ast., 18, 180
Barazza F. D., Binggeli B., Jerjen H., 2002, A&A, 391, 823
Barnes J. E., 2002, MNRAS, 333, 481
Bekki K., 1998, ApJ, 502, L133
Bekki K., 2009a, MNRAS, 398, L36
Bekki K., 2009b, MNRAS, 399, 2221
Bekki K., Tsujimoto T., Chiba M., 2009, ApJ, 692, L24
Bellstedt S., Graham A. W., Forbes D. A., Romanowsky A. J., Brodie J. P., Strader J., 2017, MNRAS, 470, 1321
Belokurov V., Erkal D., Evans N. W., Koposov S. E., Deason A. J., 2018, MNRAS, 478, 611
Bender R., 1988, A&A, 193, L7
Benson A. J., Bower R. G., Frenk C. S., Lacey C. G., Baugh C. M., Cole S., 2003, ApJ, 599, 38
Bland-Hawthorn J., Tepper-García T., 2021, MNRAS, 504, 3168
Blitz L., Robishaw T., 2000, ApJ, 541, 675
Block D. L. et al., 2007, in Combes F., Palouš J.eds, IAU Symp., vol. 235, Galaxy Evolution across the Hubble Time. Cambridge University Press, Cambridge, p. 29
Blom C., Forbes D. A., Foster C., Romanowsky A. J., Brodie J. P., 2014, MNRAS, 439, 2420
Boselli A., Gavazzi G., 2006, PASP, 118, 517
Bresolin F., 2013, ApJ, 772, L23
Brook C. B., Kawata D., Gibson B. K., Freeman K. C., 2004, ApJ, 612, 894
Brouwer M. M. et al., 2021, A&A, 650, A113
Brown D. A., Brink J., Fang H., Gair J. R., Li C., Lovelace G., Mandel I., Thorne K. S., 2007, Phys. Rev. Lett., 99, 201102
Burstein D., Ho L. C., Huchra J. P., Macri L. M., 2005, ApJ, 621, 246
Buta R. J. et al., 2015, ApJS, 217, 32
Buta R. J., 2013, in Oswalt T. D., Keel W. C., eds, Planets, Stars and Stellar Systems. Volume 6: Extragalactic Astronomy and Cosmology. Springer Science + Business Media, Dordrecht, p. 1
Buta R. J., Corwin H. G., Odewahn S. C., 2007, The de Vaucouleurs Atlas of Galaxies. Cambridge Univ. Press, Cambridge
Cameron E., Pettitt A. N., 2012, MNRAS, 425, 44
Capaccioli M., 1990, in Jarvis B., Terndrup D., eds, European Southern Observatory Conference and Workshop Proceedings, vol. 35. Garching, European Southern Observatory, p. 231
Capaccioli M., Caon N., 1992, in Longo G., Capaccioli M., Busarello G., eds, Astrophysics and Space Science Library, vol. 178, Morphological and Physical Classification of Galaxies. Kluwer Academic Publishers, Dordrecht, p. 99
Cappellari M. et al., 2011, MNRAS, 416, 1680
Capuzzo-Dolcetta R., 1993, ApJ, 415, 616
Carter D., 1978, MNRAS, 182, 797

Casey A. R. et al., 2014, MNRAS, 443, 828
Chandrasekhar S., von Neumann J., 1943, ApJ, 97, 1
Chua K. T. E., Pillepich A., Rodriguez-Gomez V., Vogelsberger M., Bird S., Hernquist L., 2017, MNRAS, 472, 4343
Ciambur B. C., 2015, ApJ, 810, 120
Ciambur B. C., Graham A. W., 2016, MNRAS, 459, 1276
Cluver M. E., Jarrett T. H., Kraan-Korteweg R. C., Koribalski B. S., Appleton P. N., Melbourne J., Emonts B., Woudt P. A., 2010, ApJ, 725, 1550
Conroy C., Wechsler R. H., Kravtsov A. V., 2007, ApJ, 668, 826
Conselice C. J., 2014, ARA&A, 52, 291
Conselice C. J., Mundy C. J., Ferreira L., Duncan K., 2022, ApJ, 940, 168
Corbin M. R., Vacca W. D., 2002, ApJ, 581, 1039
Cowie L. L., Songaila A., Hu E. M., Cohen J. G., 1996, AJ, 112, 839
Curtis H. D., 1917, PASP, 29, 206
Curtis H. D., 1918, Publ. Lick Obs., 13, 9
D'Onghia E., Springel V., Hernquist L., Keres D., 2010, ApJ, 709, 1138
D'Onghia E., Vogelsberger M., Hernquist L., 2013, ApJ, 766, 34
Daddi E. et al., 2005, ApJ, 626, 680
Damjanov I. et al., 2011, ApJ, 739, L44
Das M., O'Neil K., Vogel S. N., McGaugh S., 2006, ApJ, 651, 853
Dasyra K. M. et al., 2006, ApJ, 638, 745
Davies M. B., Miller M. C., Bellovary J. M., 2011, ApJ, 740, L42
Davis B. L., Graham A. W., Cameron E., 2018, ApJ, 869, 113
Davis B. L., Graham A. W., Cameron E., 2019, ApJ, 873, 85
Davis B. L., Graham A. W., Seigar M. S., 2017, MNRAS, 471, 2187
de Vaucouleurs G., 1959, Handbuch der Physik, 53, 275
de Vaucouleurs G., de Vaucouleurs A., Corwin J. R., 1976, Second Reference Catalogue of Bright Galaxies, 1976, 0
Dekel A. et al., 2009, Nature, 457, 451
Di Matteo P., Spite M., Haywood M., Bonifacio P., Gómez A., Spite F., Caffau E., 2020, A&A, 636, A115
Dillamore A. M., Belokurov V., Font A. S., McCarthy I. G., 2022, MNRAS, 513, 1867
Draine B. T., 2003, ARA&A, 41, 241
Draine B. T., 2004, in Blain A. W., Combes F., Draine B. T., Pfenniger D., Revaz Y.eds, The Cold Universe. Springer-Verlag, Springer Berlin Heidelberg, p. 213
Dubinski J., Gauthier J. R., Widrow L., Nickerson S., 2008, in Funes J. G., Corsini E. M., eds, ASP Conf. Ser. Vol. 396, Formation and Evolution of Galaxy Disks. Astron. Soc. Pac., San Francisco, p. 321
Ebneter K., Balick B., 1983, PASP, 95, 675
Eggen O. J., Lynden-Bell D., Sandage A. R., 1962, ApJ, 136, 748
Eingorn M., Kudinova A., Zhuk A., 2013, JCAP, 04, 010
Eldredge N., Gould S. J., 1972, in Schopf T. J., ed., Models in Paleobiology. Freeman Cooper and Company, San Francisco, CA, p. 82
Emsellem E. et al., 2011, MNRAS, 414, 888
Engelbracht C. W., Rieke G. H., Gordon K. D., Smith J. D. T., Werner M. W., Moustakas J., Willmer C. N. A., Vanzi L., 2008, ApJ, 678, 804
Engler C. et al., 2021, MNRAS, 507, 4211
Ferrarese L., Merritt D., 2000, ApJ, 539, L9
Ferreira L. et al., 2022, ApJ, 938, L2
Forbes D. A., Bridges T., 2010, MNRAS, 404, 1203
Freeman K. C., 1970, ApJ, 160, 811
Gadotti D. A., Sánchez-Janssen R., 2012, MNRAS, 423, 877
Gaia Collaboration et al., 2018, A&A, 616, A11
Gallagher J. S. I., 2010, in Smith B., Higdon J., Higdon S., Bastian N.eds, ASP Conf. Ser. Vol. 423, Galaxy Wars: Stellar Populations and Star Formation in Interacting Galaxies. Astron. Soc. Pac., San Francisco, p. 3
Gallart C., Bernard E. J., Brook C. B., Ruiz-Lara T., Cassisi S., Hill V., Monelli M., 2019, Nature Astron., 3, 932
Garling C. et al., 2018, ApJ, 852, 44
Gebhardt K. et al., 2000, ApJ, 539, L13
Goncharov B. et al., 2021, ApJ, 917, L19
Gorbachev V. I., 1970, Soviet Ast., 14, 182
Graham A. W., 2013, in Oswalt T. D., Keel W. C.eds, Planets, Stars and Stellar Systems. Volume 6: Extragalactic Astronomy and Cosmology. Springer Science + Business Media, Dordrecht, p. 91
Graham A. W., 2019a, PASA, 36, e035
Graham A. W., 2019b, MNRAS, 487, 4995
Graham A. W., 2020, MNRAS, 492, 3263
Graham A. W., 2023a, MNRAS, 518, 6293
Graham A. W., 2023b, MNRAS, 521, 1023
Graham A. W., Ciambur B. C., Savorgnan G. A. D., 2016, ApJ, 831, 132
Graham A. W., Colless M. M., Busarello G., Zaggia S., Longo G., 1998, A&AS, 133, 325
Graham A. W., Erwin P., Caon N., Trujillo I., 2001, ApJ, 563, L11
Graham A. W., Erwin P., Trujillo I., Asensio Ramos A., 2003a, AJ, 125, 2951
Graham A. W., Janz J., Penny S. J., Chilingarian I. V., Ciambur B. C., Forbes D. A., Davies R. L., 2017, ApJ, 840, 68
Graham A. W., Jerjen H., Guzmán R., 2003b, AJ, 126, 1787
Graham A. W., Sahu N., 2023a, MNRAS, 518, 2177
Graham A. W., Sahu N., 2023b, MNRAS, 520, 1975
Graham A. W., Soria R., Ciambur B. C., Davis B. L., Swartz D. A., 2021, ApJ, 923, 146
Graham A. W., Worley C. C., 2008, MNRAS, 388, 1708
Gunn J. E., Gott J., Richard I., 1972, ApJ, 176, 1
Hammer F., Flores H., Puech M., Yang Y. B., Athanassoula E., Rodrigues M., Delgado R., 2009, A&A, 507, 1313
Harikane Y. et al., 2023, ApJS, 265, 5
Hart R., Berendzen R., 1971, J. History Astron., 2, 109
Hau G. K. T., Bower R. G., Kilborn V., Forbes D. A., Balogh M. L., Oosterloo T., 2008, MNRAS, 385, 1965
Heckman T. M., Best P. N., 2014, ARA&A, 52, 589
Helmi A., Babusiaux C., Koppelman H. H., Massari D., Veljanoski J., Brown A. G. A., 2018, Nature, 563, 85
Helmi A., White S. D. M., de Zeeuw P. T., Zhao H., 1999, Nature, 402, 53
Henkel C., Javanmardi B., Martínez-Delgado D., Kroupa P., Teuwen K., 2017, A&A, 603, A18
Herschel J. F. W. S., 1847, Results of Astronomical Observations Made during the Years 1834, 5, 6, 7, 8, at the Cape of Good Hope; being the Completion of a Telescopic Survey of the Whole Surface of the Visible Heavens, Commenced in 1825. London, Smith, Elder and Co.
Hoffman G. L., Lu N. Y., Salpeter E. E., Farhat B., Lamphier C., Roos T., 1993, AJ, 106, 39
Hoffman L., Loeb A., 2006, ApJ, 638, L75
Holmberg E., 1950, Meddelanden fran Lunds Astronomiska Observatorium Serie II, 128, 5
Hopkins P. F., Hernquist L., Cox T. J., Kereš D., 2008, ApJS, 175, 356
Horta D. et al., 2021, MNRAS, 500, 1385
Hou M., Liu X., Guo H., Li Z., Shen Y., Green P. J., 2019, ApJ, 882, 41
Hoyle F., 1951, in Problems of Cosmical Aerodynamics. Proc. Symp. Motion of Gaseous Masses of Cosmical Dimensions. Central Air Documents Office (Army-Navy-Air Force), Dayton, p. 195
Hubble E. P., 1922, ApJ, 56, 162
Hubble E. P., 1926, ApJ, 64, 321
Hubble E. P., 1936, Realm of the Nebulae. Yale Univ. Press, New Haven
Hutchings J. B., Neff S. G., 1989, AJ, 97, 1306
Impey C., Bothun G., 1997, ARA&A, 35, 267
Inoue S., 2011, MNRAS, 416, 1181
Ishiyama T. et al., 2013, ApJ, 767, 146
Javanmardi B. et al., 2016, A&A, 588, A89
Jeans J. H., 1919, Problems of Cosmogony and Stellar Dynamics. Cambridge Univ. Press, Cambridge
Jeans J. H., 1928, Astronomy and Cosmogony. Cambridge Univ. Press, Cambridge
Jerjen H., Kalnajs A., Binggeli B., 2000, A&A, 358, 845
Julian W. H., Toomre A., 1966, ApJ, 146, 810
Kawata D., Baba J., Ciucă I., Cropper M., Grand R. J. J., Hunt J. A. S., Seabroke G., 2018, MNRAS, 479, L108
Kawata D., Mulchaey J. S., 2008, ApJ, 672, L103
Kazantzidis S., Zentner A. R., Kravtsov A. V., Bullock J. S., Debattista V. P., 2009, ApJ, 700, 1896
Knox-Shaw H., 1915, Helwan Institute of Astronomy and Geophysics Bulletins, 15, 129

Komossa S., Burwitz V., Hasinger G., Predehl P., Kaastra J. S., Ikebe Y., 2003, ApJ, 582, L15
Kormendy J., Bender R., 2012, ApJS, 198, 2
Kormendy J., Fisher D. B., Cornell M. E., Bender R., 2009, ApJS, 182, 216
Kormendy J., Ho L. C., 2013, ARA&A, 51, 511
Kruijssen J. M. D., Pfeffer J. L., Reina-Campos M., Crain R. A., Bastian N., 2019, MNRAS, 486, 3180
Labbé I. et al., 2023, Nature, 616, 266
Laine S., van der Marel R. P., Lauer T. R., Postman M., O'Dea C. P., Owen F. N., 2003, AJ, 125, 478
Larsen S. S., Brodie J. P., Huchra J. P., Forbes D. A., Grillmair C. J., 2001, AJ, 121, 2974
Leaman R., van de Ven G., 2022, MNRAS, 516, 4691
Li T. S. et al., 2018, ApJ, 866, 22
Liller M. H., 1966, ApJ, 146, 28
Lin C. C., Shu F. H., 1964, ApJ, 140, 646
Lundmark K., 1925, MNRAS, 85, 865
Lundmark K., 1926, Arkiv for Matematik, Astronomioch Fysik, 19, 1
Mädler J. H. v., 1846, Astron. Nachr., 24, 213
Madrid J. P., Leigh N. W. C., Hurley J. R., Giersz M., 2017, MNRAS, 470, 1729
Magorrian J. et al., 1998, AJ, 115, 2285
Mandel I., Gair J. R., 2009, Class. Quant. Gravity, 26, 094036
Mao Y.-Y., Geha M., Wechsler R. H., Weiner B., Tollerud E. J., Nadler E. O., Kallivayalil N., 2021, ApJ, 907, 85
Martínez-Delgado D. et al., 2010, AJ, 140, 962
Martínez-Delgado D., Aparicio A., Gómez-Flechoso M. Á., Carrera R., 2001, ApJ, 549, L199
Martínez-Delgado D., Peñarrubia J., Gabany R. J., Trujillo I., Majewski S. R., Pohlen M., 2008, ApJ, 689, 184
Matsuno T., Aoki W., Suda T., 2019, ApJ, 874, L35
Matthias M., Gerhard O., 1999, MNRAS, 310, 879
McGaugh S. S., 1994, ApJ, 426, 135
McNamara B. R., Nulsen P. E. J., 2012, New J. Phys., 14, 055023
Merritt D., 2006, ApJ, 648, 976
Mirabel I. F. et al., 1999, A&A, 341, 667
Mitchel O. M., 1847, Sidereal Messenger, 1, 121
Moore B., Ghigna S., Governato F., Lake G., Quinn T., Stadel J., Tozzi P., 1999, ApJ, 524, L19
Naab T., Burkert A., 2003, ApJ, 597, 893
Nieto J. L., Capaccioli M., Held E. V., 1988, A&A, 195, L1
Omar A., Dwarakanath K. S., 2005, J. Astrophys. Astron., 26, 71
Ostriker J. P., Binney J., Saha P., 1989, MNRAS, 241, 849
Park C., Gott J., Richard I., Choi Y.-Y., 2008, ApJ, 674, 784
Pickering T. E., Impey C. D., van Gorkom J. H., Bothun G. D., 1997, AJ, 114, 1858
Posti L., Fall S. M., 2021, A&A, 649, A119
Pota V. et al., 2013, MNRAS, 428, 389
Powell M. C., Urry C. M., Cardamone C. N., Simmons B. D., Schawinski K., Young S., Kawakatsu M., 2017, ApJ, 835, 22
Querejeta M. et al., 2015, A&A, 579, L2
Quinn P. J., Hernquist L., Fullagar D. P., 1993, ApJ, 403, 74
Rathore H., Kumar K., Mishra P. K., Wadadekar Y., Bait O., 2022, MNRAS, 513, 389
Reynolds J. H., 1920, MNRAS, 80, 746
Reynolds J. H., 1921, Observatory, 44, 368
Reynolds J. H., 1925, MNRAS, 85, 1014
Rix H.-W., White S. D. M., 1990, ApJ, 362, 52
Roberts I., 1895, MNRAS, 56, 70
Roche E. A., 1850, Montpellier Academy of Sciences and Letters. Mémoires de la section des sciences, 1, 333
Rosse T. E. O., 1850, Phil. Trans. R. Soc. London Ser. I, 140, 499
Runge J., Walker S. A., Mirakhor M. S., 2022, MNRAS, 509, 2647
Saglia R. P. et al., 2016, ApJ, 818, 47
Sahu N., Graham A. W., Davis B. L., 2019a, ApJ, 876, 155
Sahu N., Graham A. W., Davis B. L., 2019b, ApJ, 887, 10
Sahu N., Graham A. W., Davis B. L., 2020, ApJ, 903, 97
Salpeter E. E., 1964, ApJ, 140, 796
Sandage A., Binggeli B., 1984, AJ, 89, 919
Savorgnan G. A. D., Graham A. W., 2016, ApJS, 222, 10
Schawinski K. et al., 2014, MNRAS, 440, 889
Scheiner J., 1899, AJ, 9, 149
Schiavi R., Capuzzo-Dolcetta R., Arca-Sedda M., Spera M., 2020, A&A, 642, A30
Schombert J., 1998, AJ, 116, 1650
Searle L., Zinn R., 1978, ApJ, 225, 357
Seigar M. S., Kennefick D., Kennefick J., Lacy C. H. S., 2008, ApJ, 678, L93
Sellwood J. A., 2011, MNRAS, 410, 1637
Sérsic J. L., 1963, Boletin de la Asociacion Argentina de Astronomia La Plata Argentina, 6, 41
Shannon R. M. et al., 2015, Science, 349, 1522
Sil'chenko O. K., Afanasiev V. L., Chavushyan V. H., Valdes J. R., 2002, ApJ, 577, 668
Silk J., Rees M. J., 1998, A&A, 331, L1
Smith R. M., Martínez V. J., Fernández-Soto A., Ballesteros F. J., Ortiz-Gil A., 2008, ApJ, 679, 420
Spitzer Lyman J., Baade W., 1951, ApJ, 113, 413
Steinmetz M., Navarro J. F., 2002, New A, 7, 155
Thilker D. A. et al., 2010, ApJ, 714, L171
Toth G., Ostriker J. P., 1992, ApJ, 389, 5
Tremaine S. D., Ostriker J. P., Spitzer L. J., 1975, ApJ, 196, 407
van den Bergh S., 1976, ApJ, 206, 883
van den Bergh S., 1990, ApJ, 348, 57
van den Bergh S., 1997, AJ, 113, 2054
van den Bergh S., 2009, ApJ, 702, 1502
van den Bosch F. C., Aquino D., Yang X., Mo H. J., Pasquali A., McIntosh D. H., Weinmann S. M., Kang X., 2008, MNRAS, 387, 79
van der Marel R. P., Besla G., Cox T. J., Sohn S. T., Anderson J., 2012, ApJ, 753, 9
van Zee L., Haynes M. P., Giovanelli R., 1995, AJ, 109, 990
von Humboldt A., 1845, Kosmos: Entwurf einer physischen Weltbeschreibung. Hippolyte Bailliére, London
Wang J. et al., 2015, MNRAS, 453, 2399
Wang S. et al., 2022, ApJ, 927, 66
Way M. J., 2013, in Way M. J., Hunter D.eds, ASP Conf. Ser. Vol. 471, Origins of the Expanding Universe: 1912-1932. Astron. Soc. Pac., San Francisco, p. 97
White S. D. M., Rees M. J., 1978, MNRAS, 183, 341
Wilman D. J., Fontanot F., De Lucia G., Erwin P., Monaco P., 2013, MNRAS, 433, 2986
Wolf C. J. E., Rayet G., 1867, Academie des Sciences Paris Comptes Rendus, 65, 292
Wolf M., 1908, Publikationen des Astrophysikalischen Instituts Koenigstuhl-Heidelberg, 3, 109
Wright W. H., 1914, ApJ, 40, 466
Yagi M. et al., 2010, AJ, 140, 1814
Yuan T. et al., 2017, ApJ, 850, 61

APPENDIX A: THE $M_{\rm BH}$–$M_{*,\rm GAL}$ DIAGRAM

Fig. A1 exposes the steps for extracting the 'Triangal' (Fig. 4) from the $M_{\rm bh}$–$M_{*,\rm sph}$ diagram (Fig. 1), revealing something like a galactic family tree. This section explores the $M_{\rm bh}$–$M_{*,\rm gal}$ diagram to further witness the galaxy connections, show that the separation of the dust-poor and dust-rich S0 galaxies is not a consequence of the galaxy decomposition procedure, and establish which relations may exist without needing galaxy decompositions.

The changes when switching from the $M_{\rm bh}$–$M_{*,\rm sph}$ diagram to the $M_{\rm bh}$–$M_{*,\rm gal}$ diagram can be understood by looking at the B/T ratios. For the disc galaxies, Fig. A2 reveals the varying B/T ratios across the $M_{\rm bh}$–$M_{*,\rm sph}$ diagram and along the S0 and S sequences. For the ordinary E/ES,e galaxies and BCGs – predominantly E galaxies – the semiminor to semimajor axis size (b/a) ratios have been plotted

instead of the *B*/*T* ratios, which are close to 1. Ratios of 1.0 yield the largest circles in Fig. A2.

The offset nature of the BCGs relative to the ordinary (non-BCG) E/ES,e galaxies seen in Fig. 1 can also be seen in the $M_{\rm bh}$–$M_{*,\rm gal}$ diagram (Fig. A3, panel A). In passing, it is noted that the galaxy sample's morphological types (Graham & Sahu 2023a, b) confirm past allegations (Liller 1966; Gorbachev 1970) that most E4 and all E5, E6, and E7 designations were assigned to misclassified S0 galaxies. Given the dominance of the spheroid in BCGs and E/ES,e galaxies, the situation in panel A of Fig. A3 is similar to that seen in Fig. 1. The ordinary E/ES,e galaxies follow a near-quadratic relation given in Table 1.

In panel B of Fig. A3, the two merger-built core-Sérsic S0 galaxies, the two dusty ES,b galaxies, and the dusty (non-BCG) S0 galaxies built from major wet mergers, have been combined with the ordinary E/ES,e galaxies. Excluding the three labelled galaxies (NGC 3489, NGC 3377, and NGC 6251), these 39 non-BCGs give a relation with a logarithmic slope of 2.27 ± 0.25 (see Table 1), shown by the solid line in panel B of Fig. A3. Additionally excluding the two dusty ES,b galaxies changes the logarithmic slope to 2.30 ± 0.25 and the intercept to 8.63 ± 0.11.

In understanding the high-mass end of the $M_{\rm bh}$–$M_{*,\rm gal}$ diagram, the arrows in Fig. A3 show the pathway of dry, equal-mass mergers, which shift systems off the steeper-than-linear $M_{\rm bh}$–$M_{*,\rm gal}$ relation defined by the ordinary (pre-merged) E/ES.e galaxies. One can appreciate how the BCGs have evolved away from this relationship with a logarithmic slope of ∼2 by individually following a path with a slope of 1. Due to the different pre-merger starting points in the $M_{\rm bh}$–$M_{*,\rm gal}$ diagram, the collective merger-induced shifts can result in the BCG following an offset distribution which roughly preserves the original logarithmic slope of ∼2. Greater numbers of BCGs will help to quantify their distribution better.[16]

The sample size of nine BCG (excluding NGC 1316) is too low to obtain a reliable fit, with the Bayesian analysis giving an uncertain logarithmic slope of 3.24 ± 1.38. Therefore, the dashed lines in Fig. A3 are not a fit but simply a shift by a factor of two to a higher BH and galaxy stellar masses. Adding these nine BCG to the other galaxies built from major mergers yields the relation

$$\log(M_{\rm bh}/M_\odot) = (2.07 \pm 0.19)[\log(M_{*,\rm gal}/M_\odot) - 11.37] + (8.83 \pm 0.10), \quad \text{(A1)}$$

shown by the solid line in Fig. A4.[17] While this is not too dissimilar from the relation defined by the ordinary E/ES,e galaxies in panel A of Fig. A3, it should be remembered that equation (A1) depends on the relative number of morphological types in the sample. For example, a sample dominated by BCG would yield a relation with a lower $M_{\rm bh}/M_{*,\rm gal}$ ratio at a given mass than a sample dominated by non-BCG E/ES,e galaxies. Although the extension of equation (A1) to low masses is shown in Fig. A4, strictly speaking, equation (A1) applies, modulo the above caveat, for early-type galaxies with $M_{*,\rm gal} > (0.6\text{–}0.8) \times 10^{11}$ M$_\odot$.

Given the scatter in Fig. A4, robust regression lines were not obtained for the dust-poor S0 galaxies. However, the trend of higher *B*/*T* ratio with increasing mass (Fig. A2) must generate steeper $M_{\rm bh}$–$M_{*,\rm gal}$ relations than $M_{\rm bh}$–$M_{*,\rm sph}$ relations for each disc type. Thus the dust-rich (dust = Y) S0 galaxies should follow a steeper relation than the near-quadratic relation shown in Fig. A4. Indeed, the S galaxies are best fit with a logarithmic slope of 2.68 ± 0.46, or 3.04 ± 0.59, upon excluding the lowest mass S galaxy, Circinus. This latter slope is consistent with past results (Davis, Graham & Cameron 2018). The dust-rich S0 galaxies are best fit with a relation having a slope of 2.65 ± 0.54 (see Table 1), implying that the estimated slope of 2.70 ± 0.77 in the $M_{\rm bh}$–$M_{*,\rm sph}$ diagram may be more reliable at the lower end of the range.

Fig. A4 shows a tightening distribution when traversing from low to high masses. For instance, below ∼10^{11} M$_\odot$, relatively dry mergers of galaxies above the near quadratic relation (black line) will progress systems along a shallow path with a slope of ∼1 to reach the relation. In contrast, wet mergers of S galaxies below the relation must proceed along a path with a logarithmic slope steeper than ∼2 in order to generate the dust-rich (dust = Y) S0 galaxies. As such, in gas-rich systems, BH growth must out-pace stellar growth.

Without a significant second round, or extended bout, of star formation fuelled by metal-enriched gas (e.g. Bekki, Tsujimoto & Chiba 2009, and references therein), it is expected that the low-mass, dust-poor S0 galaxies will have a different stellar population and perhaps also a different abundance of planets (Adibekyan et al. 2012) to the S and dust-rich S0 galaxies. Although, all should share the same old foundational population. Separating the dusty and non-dusty S0 galaxies may aid studies of globular cluster systems in and around galaxies. For example, a prevalence of bi- or tri-modal populations of globular clusters in the dusty (gas-rich merger)-built S0 galaxies could reaffirm the evolutionary picture (Larsen et al. 2001; Forbes & Bridges 2010; Pota et al. 2013), especially if the dust-poor S0 galaxies are shown to display a uni-modal distribution of old, metal-poor, blue globular clusters while the dusty S0 galaxies additionally have more centrally concentrated metal-rich red globular clusters that formed during the galaxy merger. A comparison with the (dry merger)-built E galaxies may also be insightful for addressing how often the intermediary stage of ES and dusty S0 galaxies is bypassed in the evolutionary chain.

The relative dominance of thick and thin stellar discs from dust-poor S0 galaxies to S galaxies to dust-rich S0 galaxies might also hold important details to the evolutionary chain revealed through the 'Triangal'. Stellar discs might be born hot from turbulent gas clouds (*in situ* formation: Brook et al. 2004). Thin (and thick) stellar discs can be 'dynamically heated' and thickened from minor mergers (Quinn, Hernquist & Fullagar 1993), which can additionally directly deposit accreted stars into a thick(er) disc (Abadi et al. 2003; Casey et al. 2014), while the gas from such mergers and direct accretion can cool, settle to the mid-plane, and build a new thin disc of stars within which a spiral density wave might later form (Lin & Shu 1964). Gravitational perturbations from infalling satellite galaxies may also trigger the formation of a transient spiral pattern (Julian & Toomre 1966; D'Onghia, Vogelsberger & Hernquist 2013). In passing, it is interesting to note that some of the more major wet mergers, spawning dusty galaxies like Markarian 463 (Hutchings & Neff 1989), NGC 6240 (Komossa et al. 2003), and others (Hou et al. 2019), which are still in the early stage of merging, will contain two BHs for hundreds of millions of years prior to their coalescence.

The 'Triangal' disfavours the 'monolithic collapse' scenario (Eggen, Lynden-Bell & Sandage 1962) for E, S, and (now) dusty S0 galaxies. It suggests that the now-dust-poor S0 galaxies might be the only massive systems that formed that way. That is, these would be primordial galaxies. Due to 'down-sizing,' the most massive now-

[16]The Bayesian analysis produces an $M_{\rm bh}$–$M_{*,\rm sph}$ relation for the BCGs with an uncertain logarithmic slope of 2.89 ± 1.12. A higher logarithmic slope of 2.65–3.0 may signal the contribution from BCGs built from dusty S0/S galaxy mergers.

[17]Excluding the two dusty ES,b galaxies changes the logarithmic slope to 2.13 ± 0.18 and the intercept to 8.79 ± 0.10.

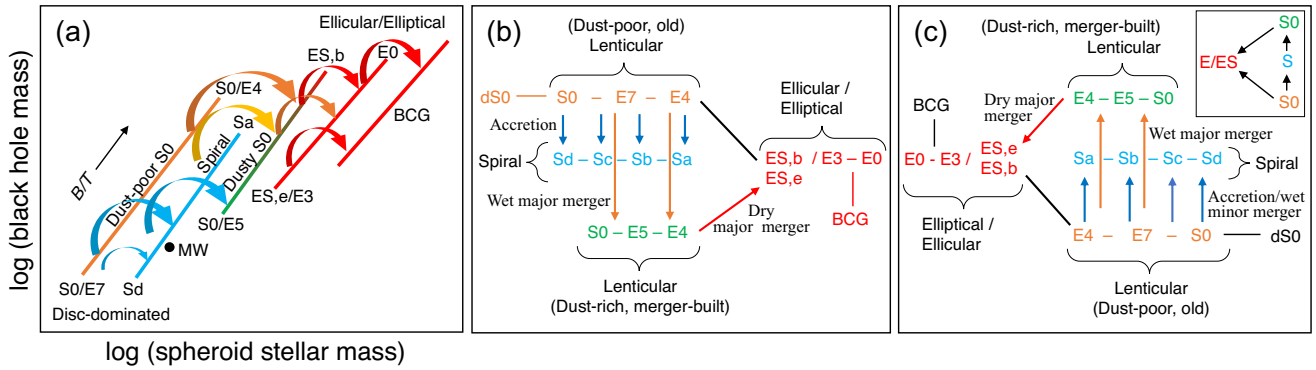

Figure A1. Sequence of galaxy evolution. Connections are revealed through the coevolution of galaxies and their BHs. The old E4 to E7 notation should be taken as representing S0 galaxies. The dusty S0 galaxies are coloured green due to their residence in the 'green valley' within the galaxy colour–luminosity diagram (Powell et al. 2017).

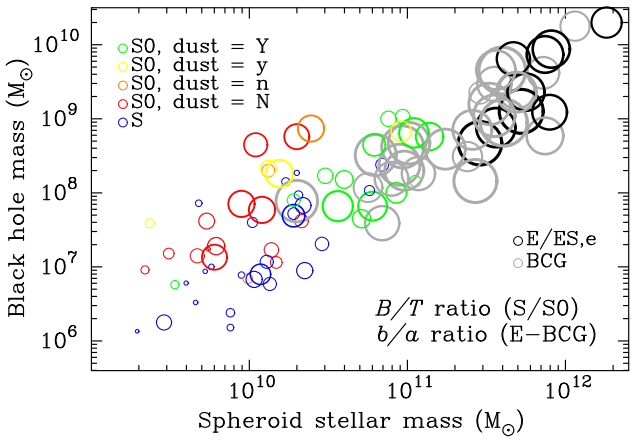

Figure A2. Ratios in the $M_{\rm bh}$–$M_{*,\rm sph}$ diagram. The symbol size linearly reflects the B/T ratios for the disc galaxies and the minor-to-major axis size (b/a) ratios for the BCG, E, and ES,e galaxies. The ratios are related to the specific angular momenta of a galaxy, the flattening and disc-dominance in E/ES/S0 galaxies, and the S galaxy morphology.

dust-poor S0 galaxies, with $M_{*,\rm sph} \sim (1–2) \times 10^{10}$ M$_\odot$ and $M_{*,\rm gal}$ of a few 10^{10} M$_\odot$, may emerge early (Harikane et al. 2023). Early major mergers in the Universe would shift these galaxies from the top-end of the now dust-poor S0 galaxy sequence to the top-end of the dust-rich S0 galaxy sequence, where some ES,b and core-Sérsic S0 galaxies reside. It is suggested here that the 10^{11} M$_\odot$ 'red nuggets' at redshifts of 2 to 3 (Daddi et al. 2005; Damjanov et al. 2011) might have formed from such mergers. An early example may be reported in Labbé et al. (2023).

The 'Triangal' reveals substantial orbital angular momentum in the Universe's first galaxies, and supports the unification of dwarf and ordinary 'early-type' galaxies (Graham 2019a, and references therein). The new galaxy sequence, encapsulated by the 'Triangal' – itself informed by the low $M_{\rm bh}/M_{*,\rm sph}$ ratios in (dry merger)–built E galaxies, core-Sérsic galaxies and BCGs that experienced 'galforming'[18]Graham & Sahu (2023b), plus the S galaxies rained down upon by satellites and significant neighbours – suggests a new hybrid galaxy evolution model. While monolithic collapse may form the (now) dust-poor S0 galaxies, accretion, and major mergers eat away at the stellar orbital angular momentum, with rising entropy building galactic bulges and spheroids. With smaller galaxies taking longer to come in from the cold, galactic speciation may be expected to first occur in the more massive systems due to the reduced mutual gravitational attraction between lower mass galaxies.

The 'Triangal' can also help paint detail onto semi-analytic simulations (Wilman et al. 2013), hierarchical models of galaxy evolution (White & Rees 1978), and cosmological N-body simulations that track mass growth but are devoid of morphological information. The trends in Figs 1 and A4 partly support the galactic metamorphosis seen in dark matter simulations that include gas and star formation (Steinmetz & Navarro 2002). However, this requires some qualification and can be regarded as 'hierarchical merging' with a couple of essential twists on the popular story. Galaxy evolution appears to differ from the headline in which S galaxies merge to form an E galaxy, which either loses its gas to become 'red and dead' (Hopkins et al. 2008, their fig.1) or experiences accretion to build a new disc Dekel et al. (2009) and possibly become an S0 or S galaxy While these things may happen, the modified picture presented here recognises that S galaxy mergers (i) form an S0 rather than an E galaxy (Barnes 2002; Naab & Burkert 2003) and (i) retain their gas. Furthermore, the more common sequence appears to be S0 to S to dust-rich S0 to E galaxy. This offers some insight into why (de Vaucouleurs, de Vaucouleurs & Corwin 1976) assigned both dusty Irregular galaxies (Irr II: Holmberg 1950) and S0/a galaxies into the same $T = 0$ numerical stage index. The Irregular galaxies had previously been positioned at the end of the galaxy sequence, after the late-type Sd/Sm spiral galaxies.

Furthermore, the 'Triangal' – which embraces elements of and captures evolutionary growth sequences not embodied in the 'Hubble sequence' or the van den Bergh trident (van den Bergh 1976; Cappellari et al. 2011) – reveals how dwarf-mass early-type galaxies are related to both ordinary (dust-poor) early-type galaxies and low-mass late-type S galaxies.[19] An emerging version of this connection can be seen in the extension of the van den Bergh trident to

[18]Some BCG and cD galaxies are expected to have such large depleted cores that a low Sérsic (1963) index function will be more practical than the core-Sérsic function (Graham et al. 2003a).

[19]The bulgeless and near-bulgeless dwarf early-type (dS0) galaxies are not displayed in the classic B/T versus morphology diagrams (Freeman 1970; Graham, Ciambur & Savorgnan 2016) due to sample selection avoiding or missing these low-mass galaxies.

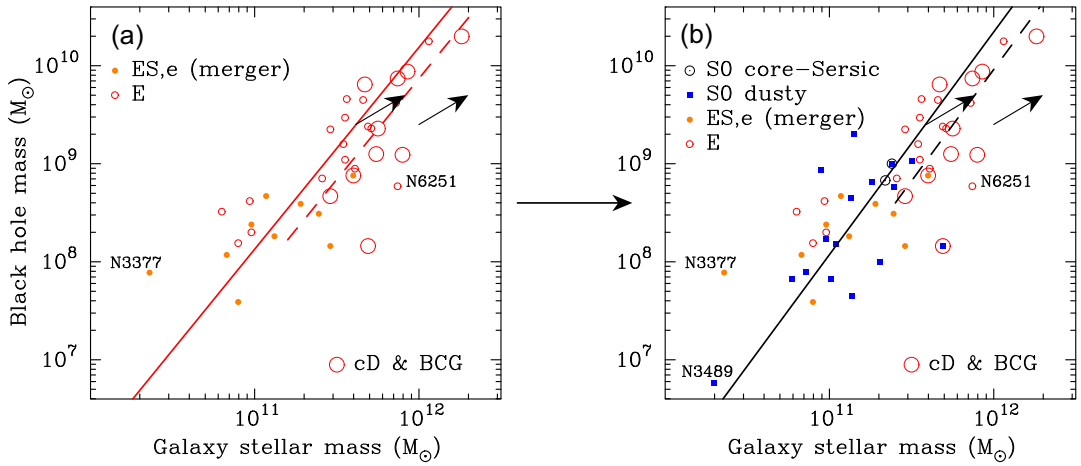

Figure A3. Merger-built galaxies in the $M_{\rm bh}$–$M_{*,\rm gal}$ diagram. Left: Fit to 24 ordinary (non-BCG) E/ES,e galaxies (excludes the labelled galaxies). The BCGs (listed in table 2 of Graham & Sahu 2023b) tend to reside to the right of the fitted relation, given in Table 1. Right: Fit to 24 non-BCG E/ES,e galaxies plus 13 dusty S0 galaxies (including two ES,b galaxies), and (two) core-Sérsic S0 galaxies. The plotted relation, provided in Table 1, has a logarithmic slope of 2.27 ± 0.25. The two dusty galaxies most above the relation are the ES,b galaxies NGC 3115 and NGC 6861, which have not grown a large-scale disc but were grouped with the S0 galaxies due to their location at the top of the S0 galaxy $M_{\rm bh}$–$M_{*,\rm sph}$ relations. The arrows have a slope of 1, representing the size of the jump induced by a major dry merger capable of creating BCGs. In both panels, the dashed line represents the ensemble of such jumps and is thus offset by $\log(2) = 0.3$ dex in both axes from the solid line.

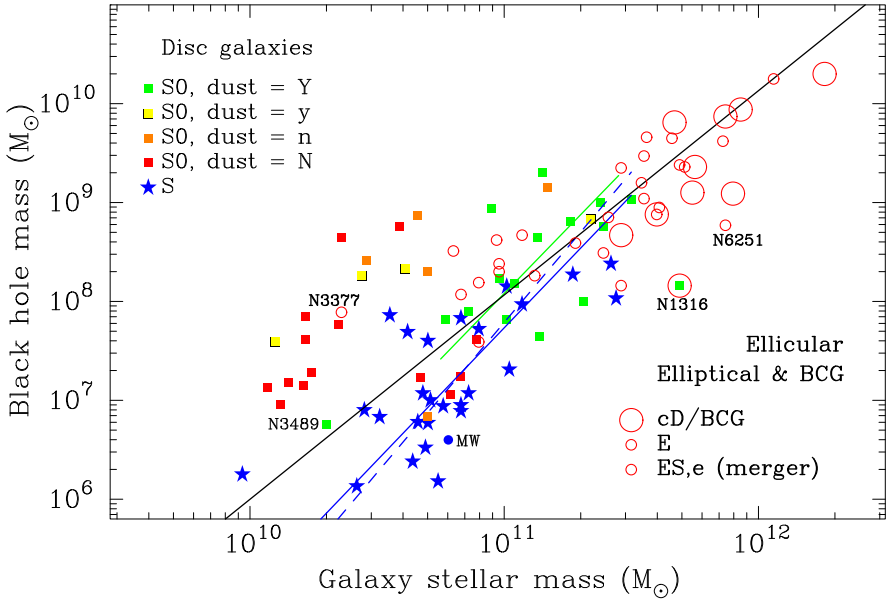

Figure A4. $M_{\rm bh}$–$M_{*,\rm gal}$ diagram. Similar to Fig. A3 but now showing all the galaxies (cf. Fig. 1). The black line, with a logarithmic slope of 2.07 ± 0.19 defined in Table 1, stems from a fit to nine cD/BCG plus 24 non-BCG E/ES,e galaxies, 14 dusty S0 galaxies (including two ES,b galaxies and one core-Sérsic S0), and a second merger-built core-Sérsic S0 galaxy but with dust = y rather than dust = Y. The labelled galaxies are excluded from the fit, as are the S galaxies and the S0 galaxies without much dust, i.e. dust = N, n, or y. This relation is defined by early-type galaxies having $M_{*,\rm gal} > (0.6\text{–}0.8) \times 10^{11}$ $M_\odot$ and is subject to sample (morphological sub-type) selection, as noted in the text. The solid blue line comes from a fit to the S galaxies, and the dashed blue line was obtained upon excluding the lowest mass S galaxy, Circinus (see Table 1).

low masses (Kormendy & Bender 2012). However, that extension did not recognise that there are two S0 galaxy sequences, that the dS0 galaxies only directly connect with one of these two sequences, or that the spirals are a bridging population between the S0 galaxies. Moreover, the alleged disjointedness (Kormendy et al. 2009; Kormendy & Bender 2012) between the dwarf and ordinary early-type galaxies has been addressed (Graham 2013, 2019a).

APPENDIX B: OUTLIERS

Possible measurement errors aside, it is not surprising to find a small number of galaxies deviating from the general trends. Infrequent events, which may be worthy of further investigation, could spawn such behaviour. In what follows, a handful of outliers have been identified for the sake of such future work. The bulk of these galaxies have previously been noted as outliers in specific

scaling diagrams, and sometimes a plausible reason has already been identified.

While the current figures do not display error bars due to the apparent clutter/confusion when displaying many galaxy types, they can be seen in Graham & Sahu (2023a).

B1 (Non-dusty) S0 galaxies

In constructing the dashed orange line in Fig. 1, the S0 galaxies with no visible dust or only a small nuclear dust ring or dust disc were regarded as non-dusty S0 galaxies. However, the non-dusty S0 galaxy NGC 4342 was excluded because it has been stripped of its stars by an unknown amount (Blom et al. 2014). Although the non-dusty S0 galaxy NGC 7457 was retained, it was previously flagged for having an unusually low 'velocity dispersion' for its BH mass (Sahu, Graham & Davis 2019b). With cylindrical rotation about its major axis, it is a likely merger remnant (Sil'chenko et al. 2002). The only other non-dusty 'S0 galaxy' to be excluded was the outlying galaxy NGC 1332, with its thin nuclear dust disc. NGC 1332 is an ES,b galaxy, which are treated as S0 galaxies in the $M_{\rm bh}$–$M_{*,\rm sph}$ diagram.

B2 S galaxies

Residing in the large Eridanus Group, the HI-deficient S galaxy NGC 1300 (Omar & Dwarakanath 2005; Wang et al. 2022) is the only S galaxy with a BH mass measurement and a (3.6 μm)-derived spheroid stellar mass that was excluded. It has either an unusually low spheroid mass or a high BH mass relative to the S galaxy $M_{\rm bh}$–$M_{*,\rm sph}$ relation (Graham 2023b).

Two bulgeless S galaxies (NGC 4395 and NGC 6926) had to be excluded due to their absence of a spheroid, and NGC 5055 still needs to have its BH mass measured. Two formerly S galaxies were reclassified as S0 galaxies: NGC 2974 and NGC 4594 (the Sombrero galaxy shown in Fig. 3).[20] This adjustment left a working sample of 25 S galaxies.

The S galaxies Circinus and NGC 2960, known to have experienced separate merger events, were retained, as was NGC 4945, the S galaxy with the lowest $M_{\rm bh}$ and $M_{*,\rm sph}$. NGC 4945 was previously flagged as an outlier in the $M_{\rm bh}$-(Sérsic n) and $M_{*,\rm sph}$–σ diagrams (Sahu, Graham & Davis 2020; Graham 2023a).

B3 Dusty S0 galaxies (wet mergers)

The $M_{\rm bh}$–$M_{*,\rm sph}$ relation for the dusty S0 galaxies is currently represented by a shift of $\Delta M_{*,\rm sph} = \log(3.5)$ from the relation for non-dusty S0 galaxies (Graham 2023b). As such, no dusty S0 galaxies are excluded from the $M_{\rm bh}$–$M_{*,\rm sph}$ diagram. However, the dusty S0 galaxies were used in the current paper to construct the $M_{\rm bh}$–$M_{*,\rm gal}$ relation for merger-built non-BCG galaxies (Fig. A3). The dusty S0 galaxies NGC 404 (outside of the plotting range in the figures) and NGC 3489 were excluded due to their location at the extremity of the distribution and, thus, their potential to bias the result defined by the other galaxies. NGC 404 ($\log(M_{\rm bh}/{\rm M}_\odot) = 5.74 \pm 0.1$ dex, $\log(M_{*,\rm gal}/{\rm M}_\odot) = 9.19 \pm 0.16$ dex) can be seen in fig. 5 of Graham & Sahu (2023a). It may be experiencing a slight rejuvenation of its stellar population (Thilker et al. 2010), or perhaps it is still experiencing the tail of star formation from a more substantial merger event (Bresolin 2013).

In Fig. A4, the dusty S0 galaxies were used in the non-BCG merger-built sample, which involved adding the E and ES,e galaxies plus the two core-Sérsic S0 galaxies in the sample. Excluded from this more extensive set were the ES,e galaxy NGC 3377, the E galaxy NGC 6251, and the S0 galaxy NGC 3489.

B4 Ordinary (non-BCG) ES and E galaxies

The ES,e galaxy NGC 3377 has the lowest spheroid mass of all ten ES galaxies in this sample. It is the only ES,e galaxy excluded due to its significant weight on the regression analysis of the ES,e/E galaxy types. NGC 3377 resides in the $M_{\rm bh}$–$M_{*,\rm sph}$ diagram (Fig. 1), where one would expect to find a dust-poor S0 galaxy. Might a large-scale disc be present, could the BH mass be in error, could NGC 3377 have been built from a relatively rare collision between disc-dominated galaxies in which the bulk of their net angular momentum happened to cancel, or perhaps something else is afoot?

NGC 6251 is the only E galaxy excluded from the sample due to its outlying nature in the $M_{\rm bh}$–$M_{*,\rm sph}$ diagram. Based on this, it may have formed from multiple galaxy mergers.

Among the non-BCG E/ES galaxies, the E galaxy NGC 1600 is flagged but retained. It is a merger remnant and the dominant galaxy in a group containing 30 faint galaxies, which has been likened to a 'fossil cluster' (Matthias & Gerhard 1999; Smith et al. 2008; Runge, Walker & Mirakhor 2022). Given its high BH and stellar mass, it too likely formed from multiple major mergers and perhaps should have been grouped with the BCGs.

NGC 3115 and NGC 6861 are dusty ES,b galaxies that have been included and excluded from the regressions. Having not grown a large-scale disc like the dusty S0 galaxies, the ES,b galaxies (Graham & Sahu 2023b) reside to the left of the $M_{\rm bh}$–$M_{*,\rm gal}$ relation defined by the non-BCG merger-built sample.

B5 BCG

Due to their low sample size of ten, a reliable linear regression was not obtained for the BCG. As such, none have been excluded *per se*, as none were used in the present regressions. However, it is noted that the Fornax cluster BCG (NGC 1316) is a dusty S0 galaxy excluded from a previous derivation of the BCG+(non-BCG) E+ES,e galaxy relation. This exclusion was because it was an S0 galaxy rather than an E or ES,e galaxy, but also due to its outlying nature in the $M_{\rm bh}$–$M_{*,\rm gal}$ scaling diagram. It appears to have been built by multiple major mergers. With BH masses around $\sim 10^9$ M$_\odot$, the BCG NGC 7768 and the non-BCG NGC 6251 are two other candidates. Such galaxies open the door to three-body encounters, which may eject one of the original BHs from the precursor galaxies (Hoffman & Loeb 2006). Of course, minor mergers may bring in a range of BHs. In passing, it is noted that while the Perseus cluster BCG NGC 1275 is an ES,e galaxy, the other eight BCGs are E galaxies.

This paper has been typeset from a TEX/LATEX file prepared by the author.

[20] As noted by Gadotti & Sánchez-Janssen (2012), NGC 4594 is sometimes described as an S galaxy within an E galaxy, as is NGC 5128 (Centaurus A: Mirabel et al. 1999), perhaps conforming with the major wet merger scenario. If spiral arms are present in NGC 4594 – although Buta et al. (2015) dispute any are – they closely resemble two rings (Bajaja et al. 1984) with a reported winding angle of just 5 degrees (Davis et al. 2017).